# THE EFFECTS OF VARIATIONS IN EXTRANEOUS COMPOSITION ON THE RELATIVE INTENSITIES EMITTED BY A CONDENSED A-C SPARK.

Kenneth B. Newbound

A thesis submitted to the Department of Physics of the University of Manitoba as a partial requirement for the degree of Master of Science, May, 1941.

# P R E F A C E

During recent years the use of spectroscopic methods of analysis has become more and more widespread. Not only are these methods used in pure research work, but they are also rapidly gaining importance in the handling of problems of analysis in industry; they have been applied in a great many fields, of which metallurgy, chemistry, criminology, medicine and biology are a few illustrative examples. The characteristics of spectroscopic methods which render their use advantageous in many problems are:

(i) they are saving of time and labor.

(ii) they require only a small sample of the material to be analysed.

(iii) they are especially suited for the determination of trace elements.

(iv) the preparation of samples for investigation is simple, often no treatment whatever being required, thus reducing the chances of contamination or loss.

(v) the maximum error is usually about 6 or 7%. (claims of higher accuracy have been made).

(vi) in some instances, particularly where the concentration of the element under examination is small, spectroscopic determinations are more reliable than those obtainable by the methods of chemistry.

While the methods in use at the present time have been successful, little is known of the phenomena occurring in electrical discharges, the most common sources of spectroscopic analysis. It is therefore desirable to learn something of these, with the aim of putting the methods on a more firmly established basis. Furthermore studies of such phenomena may be expected to lead to increased precision, reliability and sensitivity.

Part A of this work deals with the influence of extraneous composition on the relative intensities of the lines of certain elements in a standard sample, the source of excitation being a condensed a-c spark. This problem has been attacked, both from the changes in relative intensity between the spectra of different atoms, and from the changes with the spectrum of a given atom.

Other material included in this thesis has to do with the refinement and simplification of apparatus

used in spectroscopic work. A new direct reading photo-electric microphotometer has been designed and constructed through the combined efforts of Dr. G. O. Langstroth, Mr. W. W. Brown and the writer. This instrument is described in Part B.

Part C deals with an experimental investigation into the use of collimated light beams in spectrophotometry, and is based on a theoretical discussion of Dr. G. O. Langstroth. This investigation was carried out in collaboration with Mr. W. W. Brown.

The earlier parts of the thesis refer as strictly as possible to original work. Material not of immediate importance to the discussion in hand has been inserted in the form of appendices.

For the benefit of the reader who may not be acquainted with spectroscopic nomenclature, a list of terms and their significance is included in Appendix II.

## Contents.

Contents (continued).

Part A.

# Effects of Variations in the Extraneous Composition of Samples on the Intensities radiated from a Condensed A-C Spark

## Introduction

The principles underlying all modern methods of quantitative analysis by spectroscopic methods are quite general. The sample under examination is introduced into a suitable source, capable of 'exciting' the constituent atoms of the sample, so that the spectra of these atoms are radiated. Various forms of arcs or sparks are the most common light sources used in such work. Light from the source is allowed to enter the slit of a dispersing instrument, most commonly one of the forms of prism or grating spectrographs, employing a photographic means of recording the spectrum emitted by the source. A spectral line of the investigated element is chosen, and measurements are made on its intensity, usually relative to a line of another element termed an 'internal standard'. This 'internal standard' must be present in every sample in the same concentration, and may be a foreign element added to each sample or may be native to the samples. The concentration of the investigated element is then obtained from a 'working curve'. The 'working curve' is obtained from the examination under working conditions of samples containing the internal standard and the investigated

element in known concentrations. It represents the relation between relative intensity and the relative concentration of the two elements concerned.

These procedures are based on the assumption that the intensity ratio of the line of the unknown element to the line of the internal standard is a function only of their relative concentration. A number of workers have reported that the addition of an extraneous material to the sample may produce marked changes in the relative intensities.[1, 2, 3, 4, 5, 6, 7] Although such phenomena are of fundamental importance in quantitative analysis,

1. Negresco, T.J. J. chim. phys., 25:142-363. 1928.

2. Twyman, F. and Hitchen, C.S. Proc. Roy. Soc. (London) A, 133:72- . 1931.

3. Van Someren, E.H.S. J. Inst. Metals, 55:273- . 1934.

4. Duffendack, O.S., Wolfe, F.H. and Smith, H.J. Ind. Eng. Chem., Anal. Ed., 5:226- . 1933.

5. Duffendack, O.S., Wiley, F.H. and Owens, J.S. Ind. Eng. Chem., Anal. Ed., 7:410- . 1935.

6. Brode, W.R., and Appleton, J.L. Proc. 7th Spec. Conf., 36-41. 1940.

7. Brode, W.R., and Silverthorn, R.W. Proc. 6th Spec. Conf., 60-65. 1939.

with the exception of the work of Duffendack and Brode who used arc sources, no systematic study of these effects has as yet been reported.

This section of the thesis is devoted to a description of a study of the effects of extraneous composition on the relative intensities of the lines radiated from a condensed a-c spark source. The work has been based on a standard sample in the form of a solution containing lead, magnesium, and cadmium as chlorides. Loading electrodes with a constant amount of this solution, varying amounts of extraneous materials were added, and the resulting spectra studied for changes between the spectra of different elements of the standard solution, and also for variations within the spectrum of a given element. The extraneous materials used were potassium chloride, lithium chloride, calcium chloride, ammonium chloride, and boric acid.

Similar studies were made for 'buffered' solutions; that is, a large constant amount of a substance (buffer) was added to each load, and the extraneous composition varied as before. The 'buffers' used were potassium nitrate (in three different amounts) and sodium potassium tartrate; the extraneous additions being lithium chloride, calcium

chloride, and ammonium chloride.

For the greater part of the work, no condensing lens was used to focus the spark on the slit of the spectrograph; however, a few experiments were carried out with the use of such a lens, enabling a comparison of the effects to be made in these two cases.

The studies have been made with a view to determining the factors on which the effects of extraneous composition depend and means of reducing or eliminating them.

## Apparatus and Experimental Technique.

The condensed a-c spark outfit by means of which the spark was operated can be seen in the left foreground of Plate I; the electrical circuit is indicated in fig. 1.

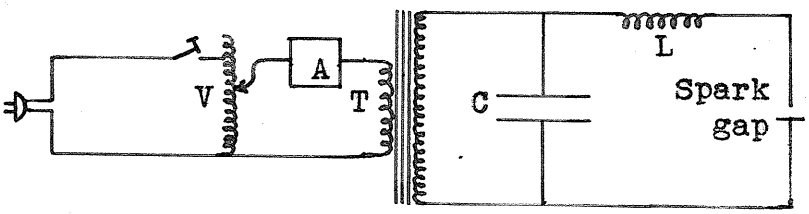


Fig. 1. Condensed a-c spark circuit diagram.

In fig. 1, V represents a General Radio 'Variac' type 200C control which allowed a continuous variation of the voltage applied to the primary of the high voltage transformer T. T, a Thordarson Transformer Type R No. 14788 is rated to supply 20,000 volts on open circuit with a 110 volt 60 cycle input. The condenser C is made up of alternating glass plates (16x16x5/8 inches) and aluminium foil. Taps are inserted to suitable layers in this condenser, permitting variation in the capacity of the circuit. The inductance L consisted of two layers of heavy, insulated copper wire wound on a $1\frac{3}{4}$ inch diameter cardboard, and soaked in

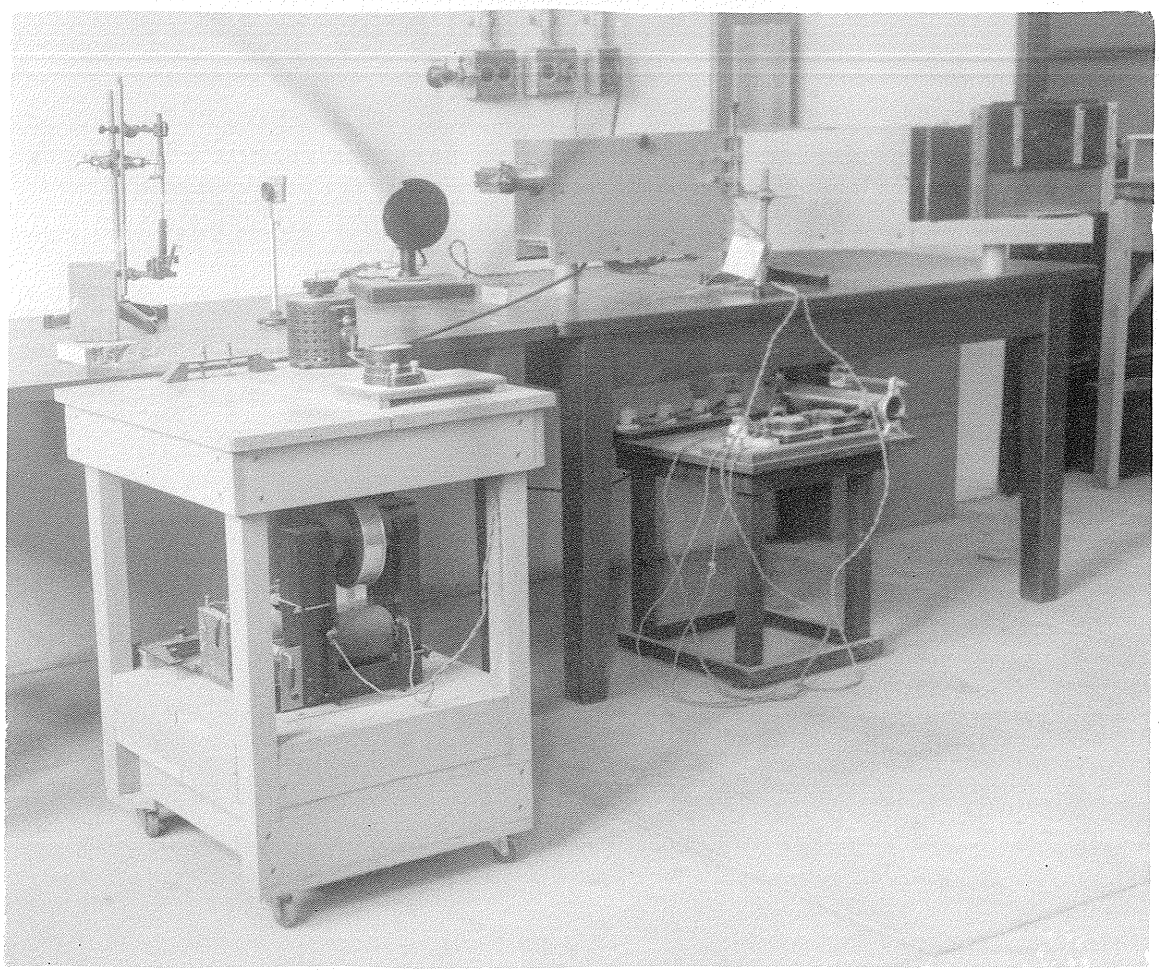

Plate I. General View of Apparatus.

Plate IIa.

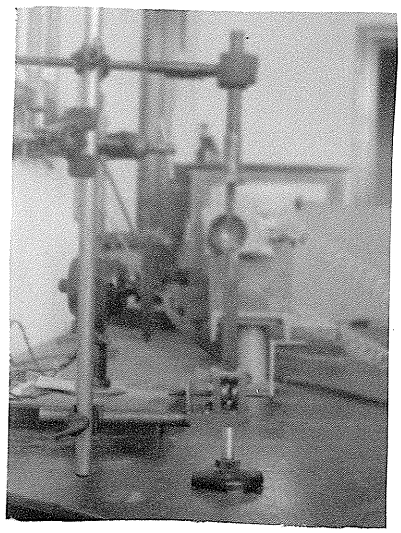

Plate IIb.

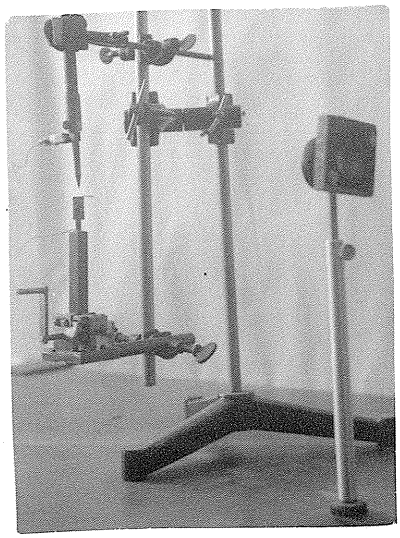

Plates II. Spark Electrode Stand.

melted paraffin wax to improve insulation. Taps inserted at appropriate points enabled the use of 37, 52 or 127 turns. It was found experimentally that a capacity of 0.03 microfarads and an inductance of 120 microhenries (127 turns) were the most satisfactory as regards the steadiness and reproducibility of the spark.

The solution employed as a standard sample throughout the experiments contained magnesium, cadmium, and lead chlorides in the following amounts: 0.000125 gm. of magnesium; 0.00100 gm. of cadmium; and 0.00100 gm. of lead per cc. A constant amount of this standard sample (0.050 cc.) was used in each load and the extraneous composition of the load varied. Five extraneous materials were used, namely: potassium chloride in amounts from 0 to 0.0064 gm. per cc. of potassium; lithium chloride to 0.00128 gm. per cc. of lithium; boric acid to 0.0018 gm. per cc. of boron; calcium chloride to 0.0064 gm. per cc. of calcium; and ammonium chloride to 0.00875 gm. per cc. of ammonium chloride. The amounts of the added compounds were such that the changes in extraneous composition involved approximately the same numbers of molecules of each.

In order to study the effects of 'buffered' solutions, a large constant amount of a substance (buffer) was added to loads containing lithium chloride, calcium chloride and ammonium chloride as extraneous materials. The buffers used were: potassium nitrate in three concentrations, viz. 0.0064 gm. per cc. of potassium, 0.0128 gm/cc., and 0.0256 gm. per cc.; and sodium potassium tartrate in a concentration of 0.0128 gm/cc. of potassium, i.e. 0.00755 gm. per cc. of sodium.

The upper electrode of the spark consisted of a pointed copper rod, while the lower plane electrodes were 'L'-shaped pieces of 24 gauge sheet copper with a sparking surface area of 1.2x1.0 cm. These electrodes were cleaned for use by dipping for a few seconds in concentrated nitric acid, then rinsing with distilled water, and finally drying by the flame from a pyrex bunsen burner, care being taken that the sparking surfaces did not enter the flame.

The cleaned plane electrodes were loaded from pipettes with 0.050 cc. of the solutions necessary to give the desired load, and were then dried in vacuo. Electrodes on which the load had dried unevenly or in large crystals were rejected. There was a marked tendency for a ring of

material to form around the edges of the electrode in all cases, except where sodium potassium tartrate was used as a buffer. In these cases, the load presented a glassy appearance and a slightly convex surface.

The loaded plane electrode and the cleaned pointed electrode were mounted in the spark holder (Plate I, upper left corner; and Plates II) and the wires from the spark outfit attached. A standard electrode separation of 3.1 mm. was used. This separation was measured by placing an incandescent lamp behind the electrodes and focussing an image of the electrodes on the slit of the spectrograph by means of a 15.0 cm. focal length f:4 quartz-fluorite achromatic lens placed on the optic axis of the spectrograph and 57.5 cm. from the slit. This same lens served as a condensing lens when it was desired to focus the spark on the slit. For such use four screens were placed over it in order to reduce the light intensity sufficiently to require an exposure time of 15 seconds. The use of screens for such a purpose is justified by the results of an investigation by Harrison.[8] The

8. Harrison, G.R. J. Optical Soc. Am. and Rev. Sci. Inst., 18:492-502. 1929.

spectrograph used was a 'medium' quartz instrument (see Appendix IV) which enabled a spectrum ranging in wavelength from 2100 Å to 6000Å to be photographed on a 4x10 inch plate. For convenience in making exposures, it was equipped with a shutter immediately behind the slit, in addition to the dark slide of the plate holder.

The procedure involved in making an exposure was as follows. The potential across the spark gap was increased until a steady spark resulted. Exposures of 15 seconds were used for unbuffered loads, while exposures of 20 to 25 seconds were required for buffered loads. During such exposures, the width of slit used corresponded to 39 on the drum.

During the exposure, the plane electrode was kept in constant horizontal motion with respect to the upper electrode, by means of an arrangement of a crank, screw and eccentric, such that the spark traced out a multiple 'W' pattern on the electrode. The rate of the motion was regulated so that the spark covered the entire electrode surface during the exposure. From seven to twelve such exposures were put on each photographic plate (see Plate III.).

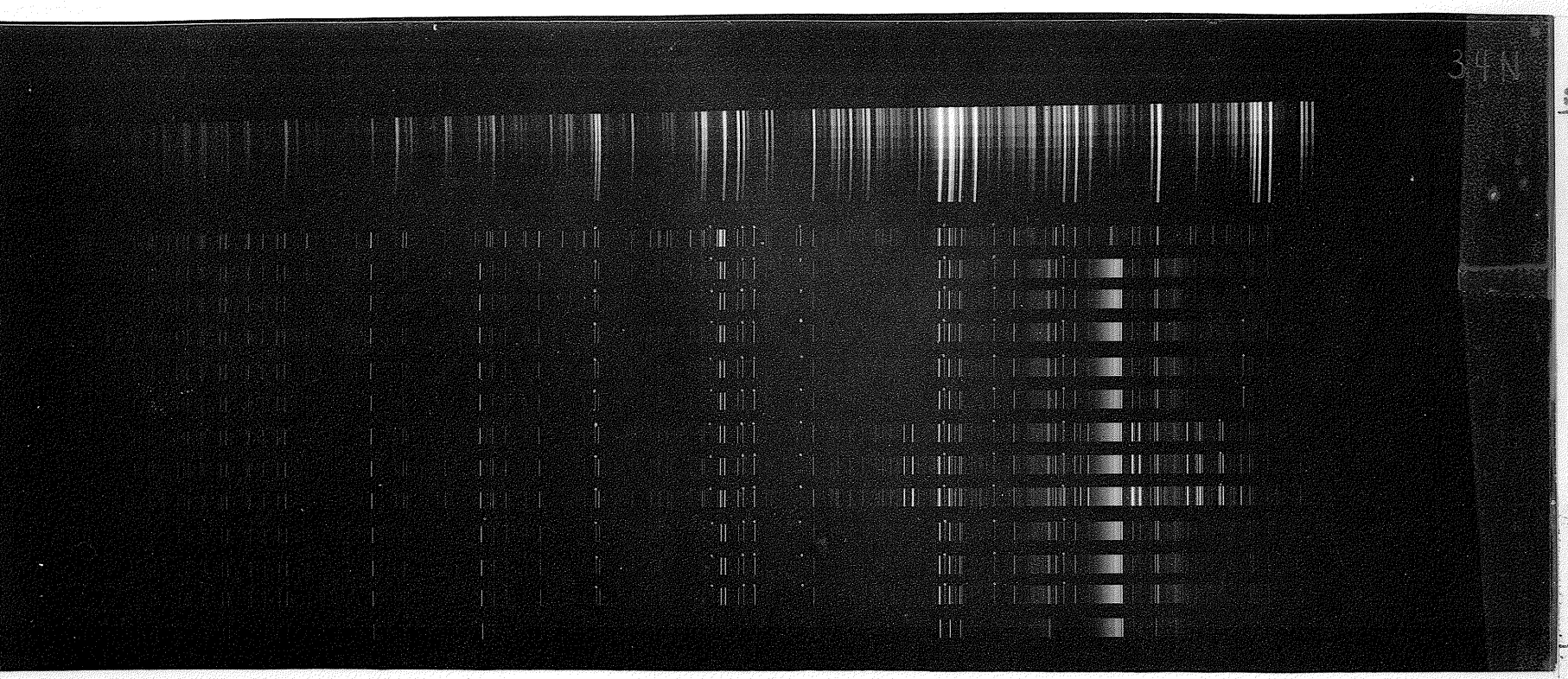

Plate III

| Decker Setting | Exposure time | Characteristics of Source |
|---|---|---|
| 1 | 7 sec. | Standard brass arc, step sector rotated immediately befo slit. (calibration marks). |
| 2 | 15 | Spark, Cu electrodes loaded with S |
| 2 | 25 | " " " " " S ≠ B. |
| 3 | 25 | " " " " " S(0.00016 gm.Li/cc.) ≠B |
| 3 | 25 | " " " " " S(0.00032 gm.Li/cc.) ≠B |
| 4 | 25 | " " " " " S(0.00064 gm.Li/cc.) ≠B |
| 4 | 25 | " " " " " S(0.00128 gm.Li/cc.) ≠B |
| 5 | 25 | " " " " " S(0.0016 gm.Ca/cc.) ≠ B |
| 5 | 25 | " " " " " S(0.0032 gm.Ca/cc.) ≠ B |
| 6 | 25 | " " " " " S(0.0064 gm.Ca/cc.) ≠ B |
| 6 | 25 | " " " " " S(0.00217 gm.N*/cc.) ≠B |
| 6 | 25 | " " " " " S(0.00438 gm N*/cc.) ≠B |
| 7 | 25 | " " " " " S(0.00875 gm.N*/cc.) ≠B |
| 7 | 25 | " " " " " B |
| 8 | 25 | |

Key to plate number 34.

Symbols used: S ≡ 0.050 cc. of standard solution, containing $MgCl_2$, $CdCl_2$, and $PbCl_2$, in concentrations of 0.000125 gm./cc. of Mg, 0.00100 gm./cc. of Cd, and 0.00100 gm./cc. of Pb.

B ≡ 0.050 cc. of NaKT buffer solution, containing 0.0128 gm./cc. of K, and 0.00755 gm./cc. of Na.

N* ≡ $NH_4Cl$.

Calibration marks were put on each plate (see Plate III) by a sector—arc method. The ordinary circuit for a d-c arc was used, the arc being run at all times under the same conditions, viz. an arc current of 3.0 amps. and an electrode separation of 1/8 inch. The electrodes were pieces of 3/16 inch brass rod. This standard arc was placed at a distance of 120 cm. from the spectrograph slit and on the optic axis of the instrument, and a step sector was rotated immediately before the slit. Exposures of from 5 to 7 seconds were taken with a slit width corresponding to 28 divisions on the drum. The step sector was made from sheet aluminium painted black, the steps transmitting 6.15, 9.50, 13.1, 19.0, 32.0, 50.0, and 100.0 % of the incident light. Rotation was secured by mounting on the shaft of a Moore Electric Corporation 115 volt a-c motor No.81650. The stand on which this motor was mounted was provided with vertical and rotational adjustments.

The photographic plates used throughout the experiments, 4x10 inch Eastman '40' Spectroscopic Plates, were developed for four minutes in D61a developer, fixed for twenty to thirty minutes in an acid hardening fixing

bath, washed for at least thirty minutes in a bath of running tap water, rinsed with distilled water, and dried.

The intensities of the spectral lines were measured on the direct reading photoelectric microphotometer, described in Part B of this thesis.

# Data and Discussion.

## Data and Discussion

Owing to the large amount of data accumulated during these experiments (over twenty five plates have been taken and studied), only typical results are being reproduced in this thesis. For ease of comparison, these are in the form of graphs.

For ease in the comparison of the different sets of intensity ratios, the ratios obtained from the unbuffered standard solution without extraneous additions have been reduced in all cases to an arbitrary value of unity, the other ratios being reduced in proportion. Provided the two lines concerned in a given ratio did not differ in wavelength by more than about 100 Å, a single calibration curve could be used in the measurements on both intensities. The resulting intensity ratios were found to be reproducible from one plate to another. For instance, for thirteen exposures using loads of unbuffered standard solution with no additions, the intensity ratios PbI 2833/MgI 2852 were found to have an average variation from the mean of 7.6%, and a maximum deviation of 15%.

In order to compare intensity ratios where the wavelength separation of the lines was more than about 100

Å, that is where two calibration curves were used, the two curves were adjusted until the central points of the straight portions of the curves coincided. Provided the two curves in question are parallel in a given density region, such procedure is equivalent to multiplying the intensities (which are only relative, in any case) of one of the curves by a constant factor, the intensity being plotted on a logarithmic scale. Due to the fact that the curves were not, in general, parallel, values taken from different plates showed average errors of about 10%, and occasional variations of as much as 25% from the mean.

Regarding the average and maximum deviations from the mean quoted above as giving an indication as to error, it may be concluded, that for the data from a given plate the probable error of a given ratio as compared with other ratios from the same plate, is about 7%, and the corresponding maximum error about 15%. In the comparison of ratios from different plates, the probable error may be somewhat higher depending on whether or not the same calibration curve was used to measure the intensities of the two lines of the ratio.

Errors in the work might arise from many sources, such as conditions of the load, variation in sparking conditions, non-uniformity of the photographic emulsion, and the photometering. To reduce these, the following precautions were taken:

(i) electrodes on which the load had dried unevenly or in large crystals were rejected.

(ii) a standard electrode separation was used, and the position of the spark with respect to the spectrograph standardised.

(iii) the potential across the spark gap was gradually increased until a steady spark was just obtained (the resistance of air breaks down at a potential essentially constant for a constant electrode separation).

(iv) for the greater part of the work, no condensing lens was used to focus the spark on the spectrograph slit; consequently the latter was uniformly illuminated and the resulting lines were uniform. In photometering such lines, both top and bottom of the line were measured, the mean value being taken if there was good agreement; otherwise, the line was examined for faults in the plate, and if such were found, the affected value or values rejected.

(v) to minimise Eberhard effects (see Appendix V) in

the lines, the developing solution was kept in constant agitation over the plate by a continual rocking motion.

The use of sodium potassium tartrate as a buffer leads to some error in the intensity measurement of the magnesium resonance line ($\lambda$ = 2852.13 Å), since there is a blend between this line and the sodium lines of wavelengths 2852.8 and 2853.0 Å. The latter lines were very faint when a load of sodium potassium tartrate was examined (see last spectrum of Plate III). It does not necessarily follow that they would be as faint, however, when other materials were present in the sample.[22] It is believed, however, that any error which may arise from this source will always be in the same direction, and the variations which may arise in the sodium line will be small compared with variations arising in the magnesium line.

Graphs I—VI represent the changes in inter spectra ratios as extraneous composition is varied. Graphs VII—XI represent the corresponding changes in intra spectrum ratios. With the exceptions of Graphs VIb, VIc, IXb, IXc, the ratios are derived from data obtained without the use of the condensing lens to focus the spark on the spectrograph slit. In the cases where

22. Webb, D.A., Nature, 139:248, 1937.

no condensing lens was used, the plotted points represent the mean values of at least two ratios (obtained by photometering both top and bottom of the lines). In many cases the points represent the mean values of two or more entirely independent exposures. In the cases where a condensing lens was used, the tops and bottoms of the lines were photometered, giving data on the spectra emitted from two points on the axis of the spark, one near the plane electrode, and the other near the pointed electrode. Intensity ratios from both of these points are presented in Graphs VI and IX.

Partial energy level diagrams of the three elements used in the standard sample are reproduced in fig. 2. The numbers to the left of each diagram are the wavenumbers corresponding to the energies of the levels, while the symbols on the right indicate the kind of level (see appendix II). The vertical lines indicate the transitions which give rise to the lines studied. The numbers along the vertical lines give the wavelength of the line in Å.

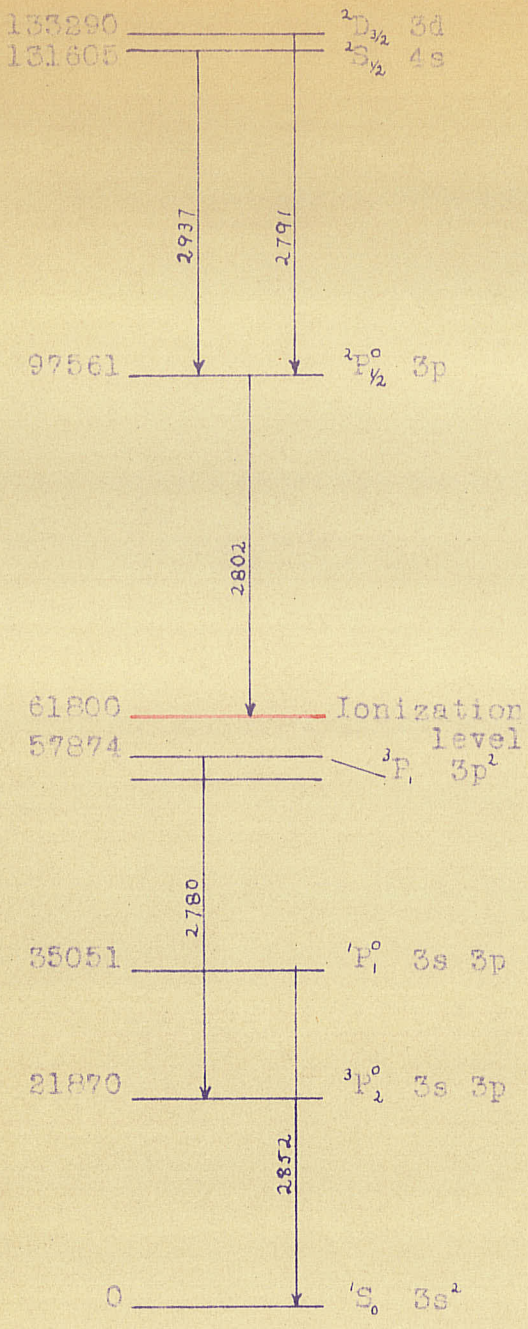


Energy Level Diagram of ionized and unionized Magnesium.

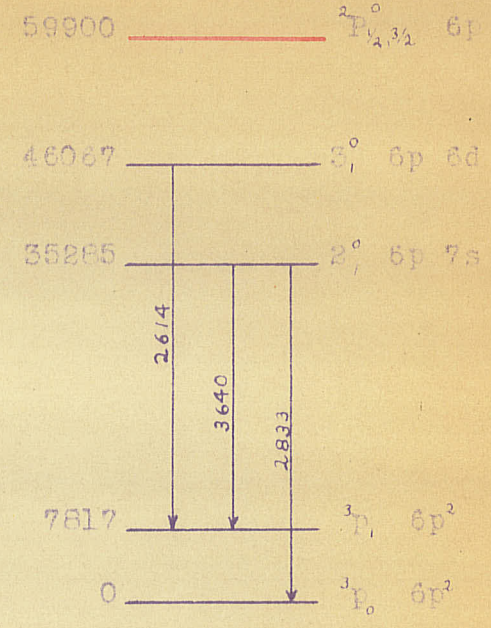


Energy Level Diagram of Unionized Lead.

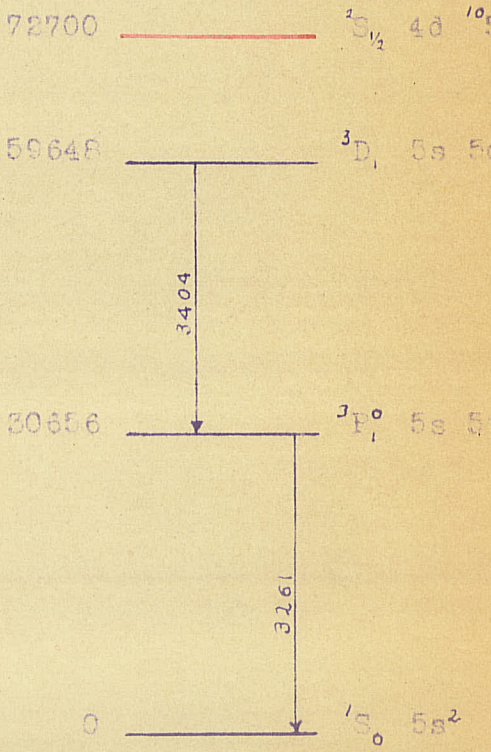


Energy Level Diagram of Unionized Cadmium.

Fig. 2. Partial Energy Level Diagrams of Elements used in Standard Solution.

The column of numbers to the left of the diagrams indicates the wave-number corresponding to the energy level. Vertical lines indicate transitions giving rise to lines studied in

# Inter Spectra Ratios

Effects of variations in extraneous composition on the intensity ratios of unbuffered solutions.

In the Graphs I, the ratios of the resonance lines of lead and cadmium to the resonance line of magnesium are plotted against extraneous composition. These graphs show clearly that the ratios do depend on the extraneous composition of the sample.

The changes in the ratios with additions of potassium chloride are not marked (see Graph Ia.), while with additions of boric acid (Graph Ib.), the changes are very marked. The larger additions of both boric acid and ammonium chloride (see Graph Ie.) were found to reduce the reproducibility of the ratios (variations of about 25% and 15% respectively were found).

It may be noted that the ratios seem to approach a constant value with the larger additions of calcium chloride (see Graph Id.); the lead to magnesium ratios act similarly for additions of lithium chloride (Graph Ic.). In these cases then, the ratios can be stabilized by the additions of large amounts of the extraneous material. This fact is the basis of the 'method of excess' proposed by Duffendack, Wiley and Owens.[5] However, for the range

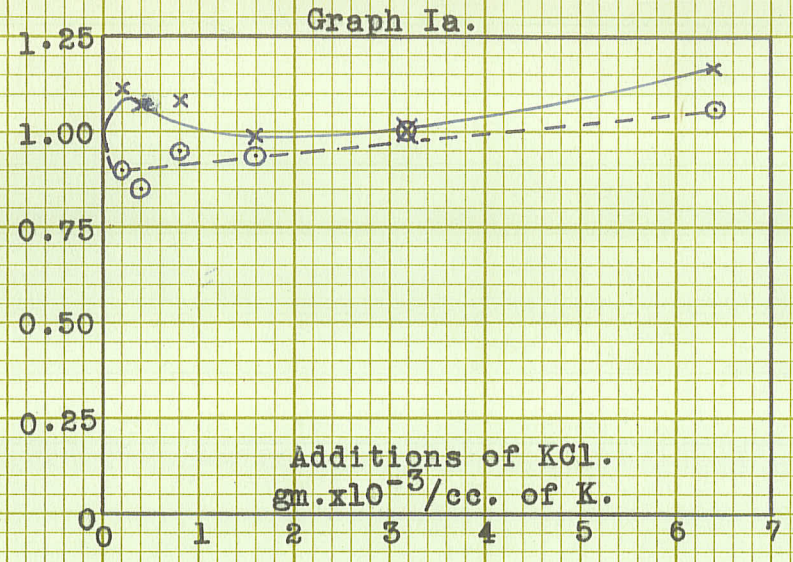


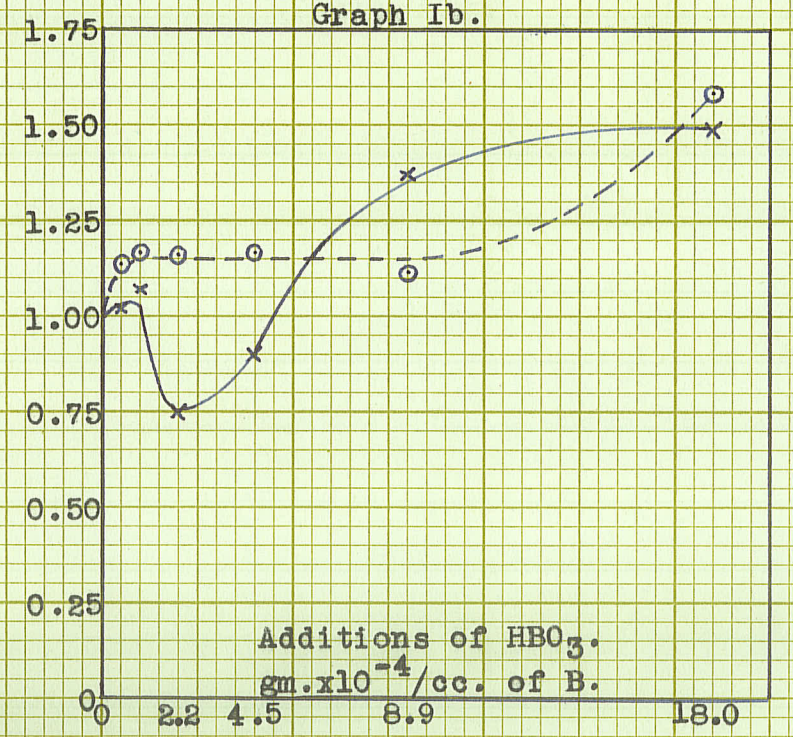


Graphs I.

Variations of Inter Element Intensity Ratios for Unbuffered Solutions, with Additions of Extraneous Materials.

⊙--⊙ PbI 2833/MgI 2852.

×——× CdI 3261/MgI 2852.

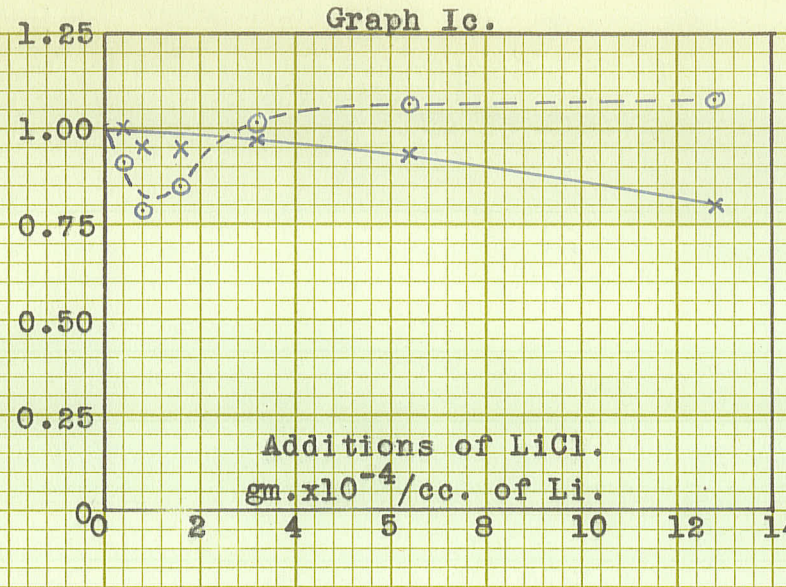


Graphs I. (cont'd.)

Variations of Inter Element Intensity Ratios for Unbuffered Solutions, with Additions of Extraneous Materials.

⊙--⊙ PbI 2833/MgI 2852.

× — × CdI 3261/MgI 2852.

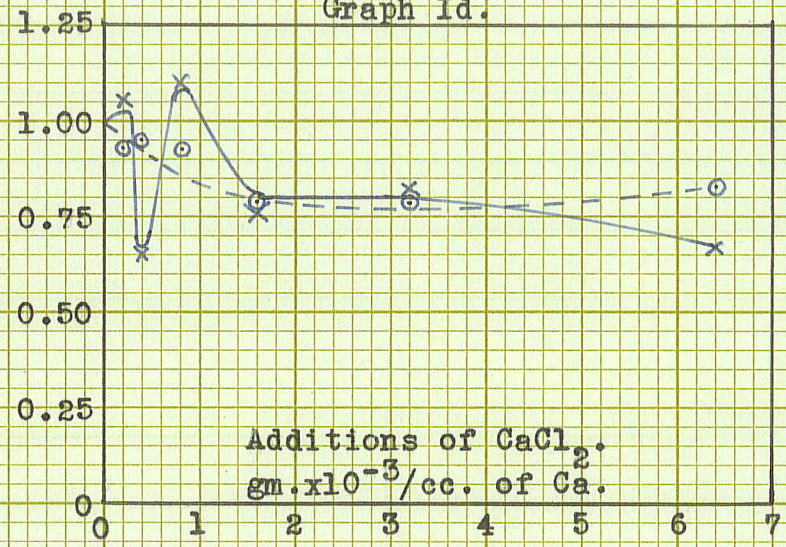


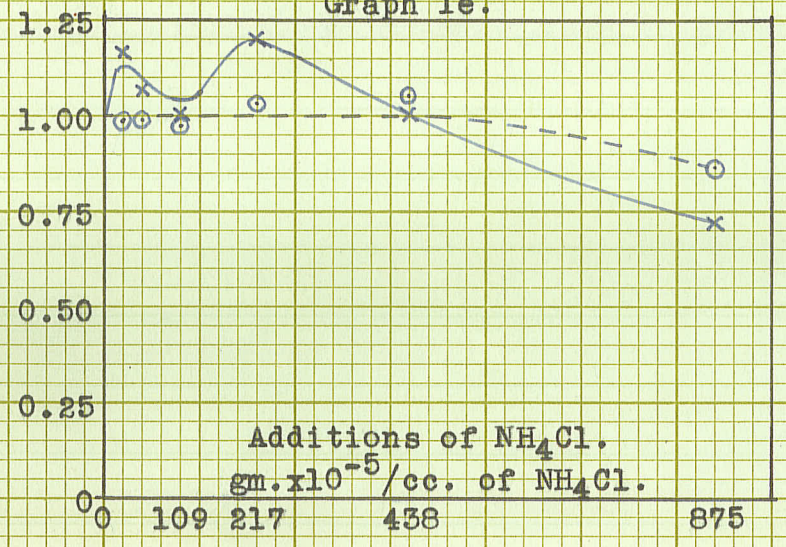

of concentrations of the additions made during these experiments, the ratios do not all approach stable values for the larger additions. This suggests that some care should be observed in applying the 'method of excess' indiscriminately.

No clear-cut correlation between the ionization potential of the addition and the effects produced by the addition is apparent from the data. The ionization potentials of the elements present in the various additions are: potassium, 4.32 volts; lithium 5.37 volts; calcium, 6.09 volts; boron 8.28 volts; chlorine, 12.96 volts. In general, the changes in the ratios with additions appear to be least when the ionization potential of the extraneous addition is least.

Efforts to correlate the effects produced by an addition with the physical characteristics of that addition (atomic weight, boiling point, etc.) have not thus far been successful.

In general, then, it may be concluded that variations in the amount of extraneous material present in an unbuffered sample, may cause marked changes in the

intensity ratios of the spectral lines of elements already present in the unbuffered sample. No correlation has been found between the effects produced by a particular addition and the ionization potential or other physical constants of the addition. While the intensity ratios may approach stable values as larger additions are made, this has not been observed in all cases within the limits of the concentrations of the extraneous materials used during these experiments.

Effects of variations in extraneous composition on the intensity ratios of solutions buffered with equivalent amounts of different substances.

In the Graphs II and III, the ratios respectively of the resonance lines of cadmium and of lead with respect to the resonance line of magnesium, are plotted against extraneous composition. Curves showing the changes in the intensity ratios of unbuffered solutions, of solutions buffered with potassium nitrate (0.0128 gm. per cc. of potassium), and of solutions buffered with sodium potassium tartrate (0.0128 gm. per cc. of potassium, 0.00755 gm. per cc. of sodium) with variation in the extraneous composition of the sample, are included on one graph for each added extraneous substance.

It is clear from the graphs that the buffers, in the amounts used in these experiments, do not improve the constancy of the lead to magnesium ratios with variation in extraneous composition. On the other hand, the constancy of the cadmium to magnesium ratios is definitely improved by the use of a buffer; the sodium potassium tartrate being in general a more effective stabilizer than the potassium

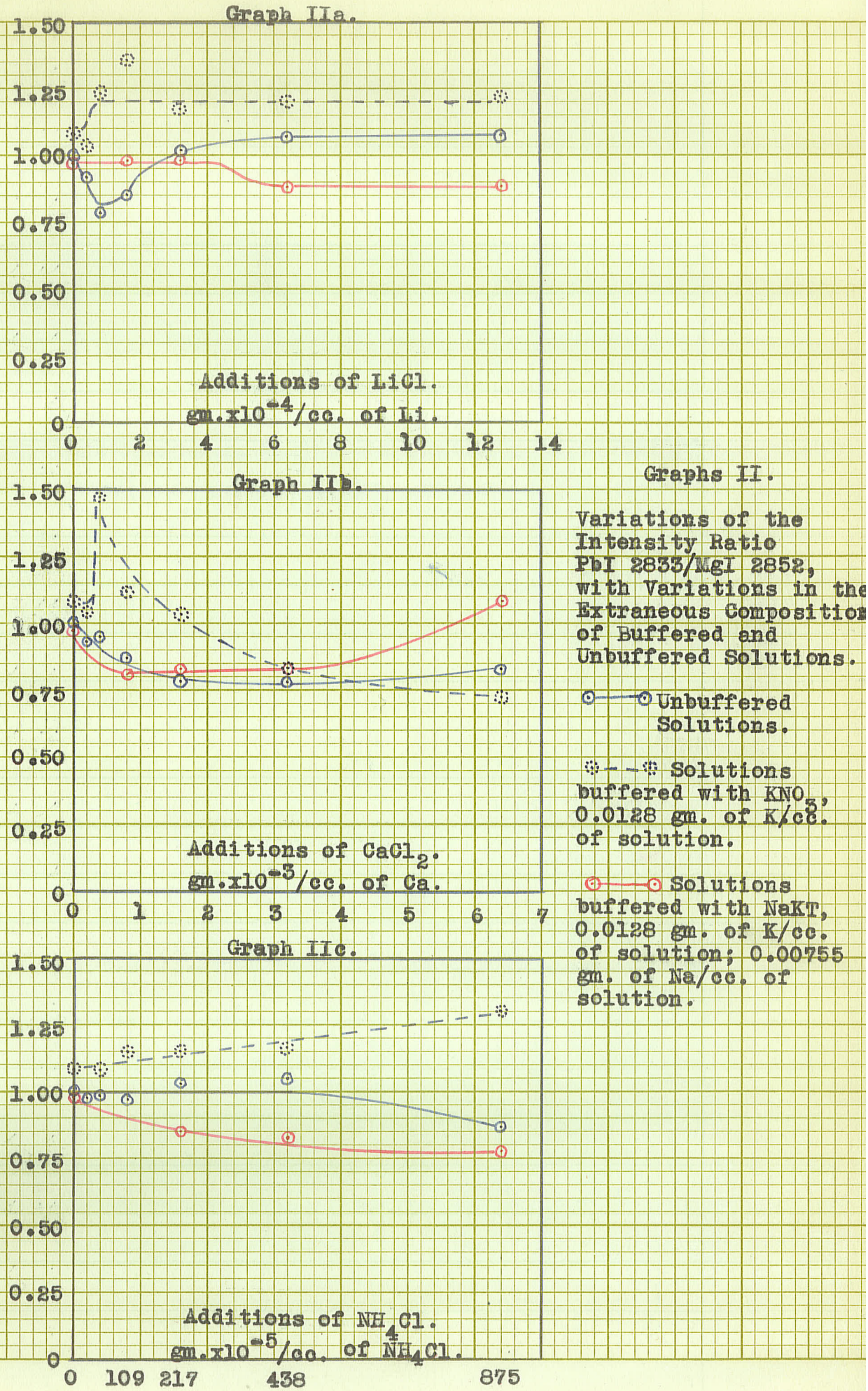


Graphs II.

Variations of the Intensity Ratio PbI 2833/MgI 2852, with Variations in the Extraneous Composition of Buffered and Unbuffered Solutions.

⊙——⊙ Unbuffered Solutions.

⊙- -⊙ Solutions buffered with $KNO_3$, 0.0128 gm. of K/cc. of solution.

⊙——⊙ Solutions buffered with NaKT, 0.0128 gm. of K/cc. of solution; 0.00755 gm. of Na/cc. of solution.

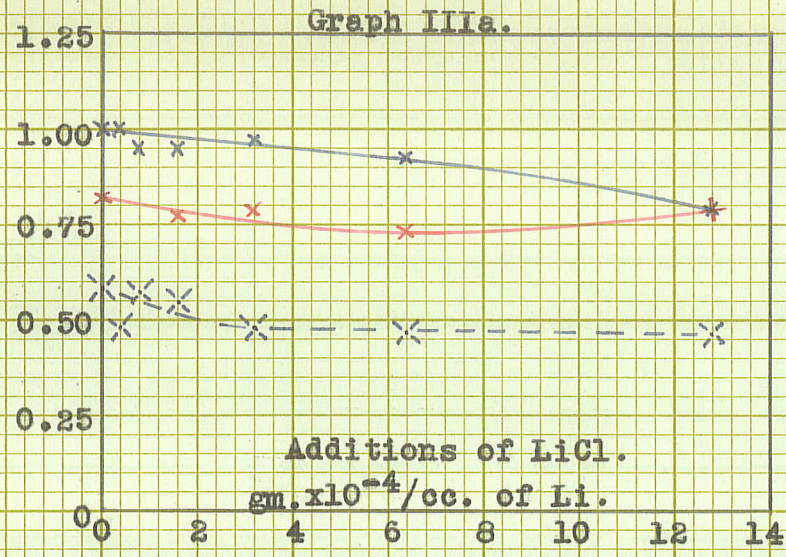


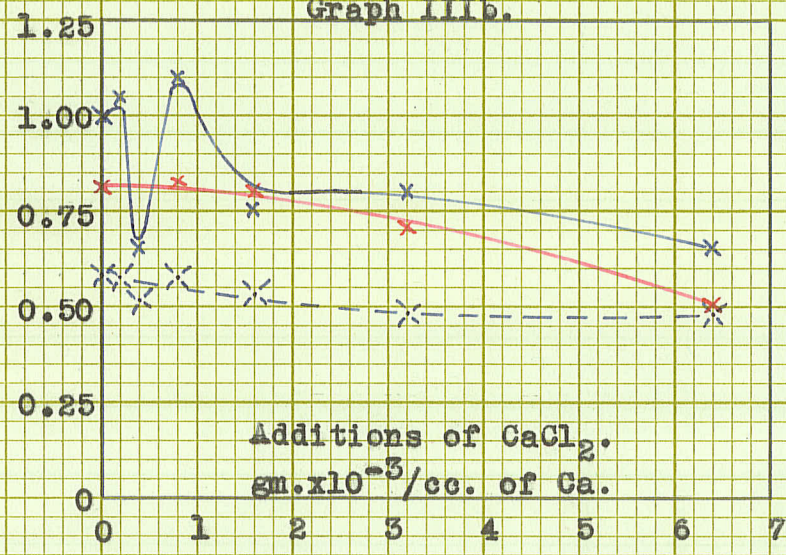


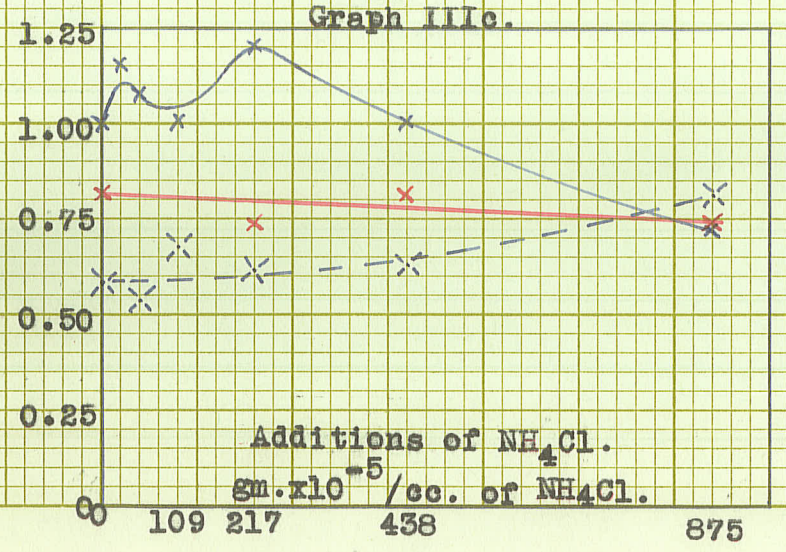


Graphs III.

Variations of the Intensity Ratio CdI 3261/MgI 2852, with Variations in the Extraneous Composition of Buffered and Unbuffered Solutions.

×——× Unbuffered Solutions.

×- -× Solutions buffered with $KNO_3$, 0.0128 gm. of K/cc. of solution.

×——× Solutions buffered with NaKT, 0.0128 gm. of K/cc. of solution; 0.00755 gm. of Na/cc. of solution.

nitrate.

In general, the behaviour of the intensity ratio of the spectral lines of two given elements with variation in extraneous composition of the sample, depends on the kind of buffer used in the sample.

From the experiments here described, it is concluded that the principle advantage in the use of a buffer, such as used in this work, lies in the increased reproducibility of the intensity ratios of the lines of the elements of the sample.

Effects of variations in extraneous composition on the intensity ratios of solutions buffered with different amounts of the same substance.

In the Graphs IV and V, the ratios of the resonance lines respectively of lead and of cadmium to the resonance line of magnesium, are plotted against extraneous composition. For each extraneous substance, there are included on one set of axes, four curves, each representing samples to which a given amount of buffer has been added, viz. unbuffered solutions, solutions buffered with potassium nitrate in three different amounts, 0.0064 gm. per cc. of potassium, 0.0128 gm. per cc. of potassium, and 0.0256 gm. per cc. of potassium.

From an inspection of Graphs IV, it appears that the use of a buffer in the form of potassium nitrate over the concentration range of the experiments, does not aid in stabilizing the lead to magnesium ratios with variation in extraneous composition.

On the other hand, the curves of the Graphs V show that the use of potassium nitrate as a buffer, has in general a stabilizing effect on the cadmium to magnesium ratios with variation in extraneous composition.

From Graph Vc, it appears that the amount of

Graph IVa.

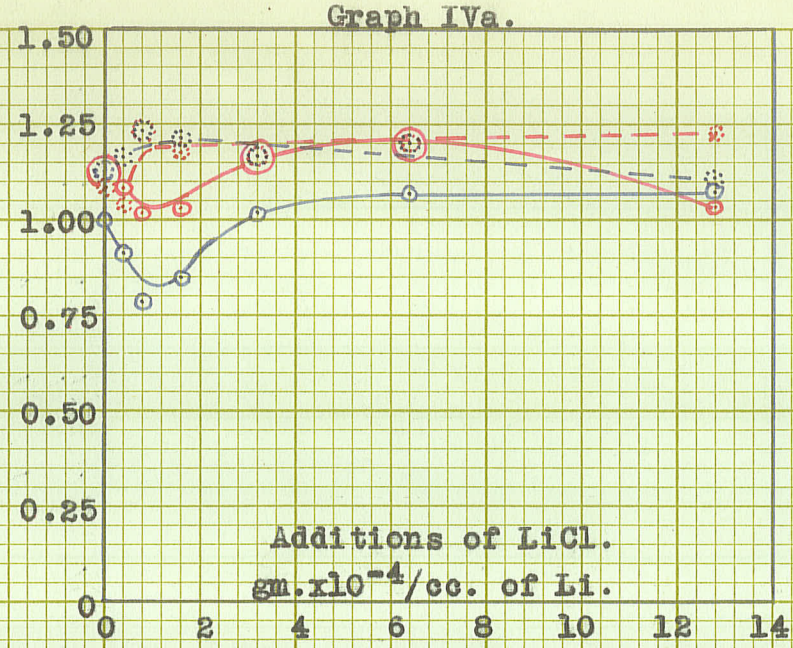


Graph IVb.

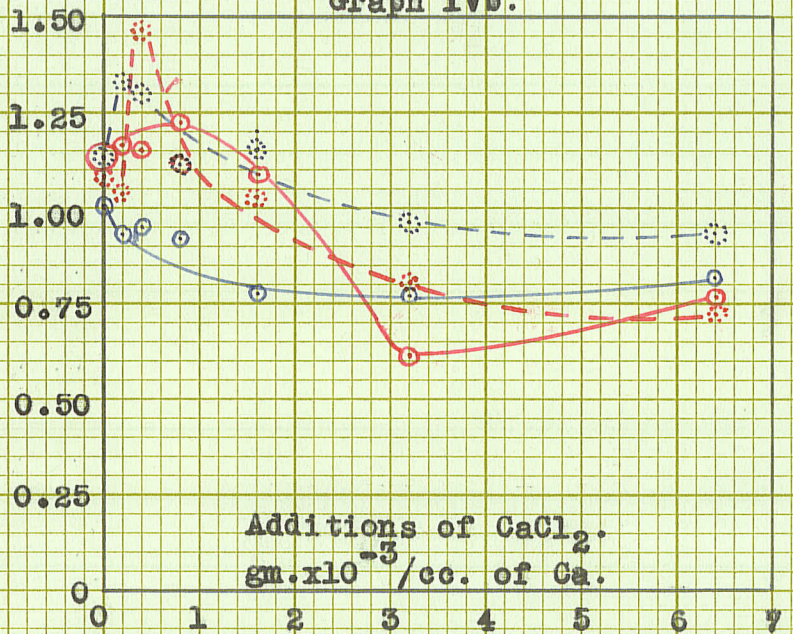


Graph IVc.

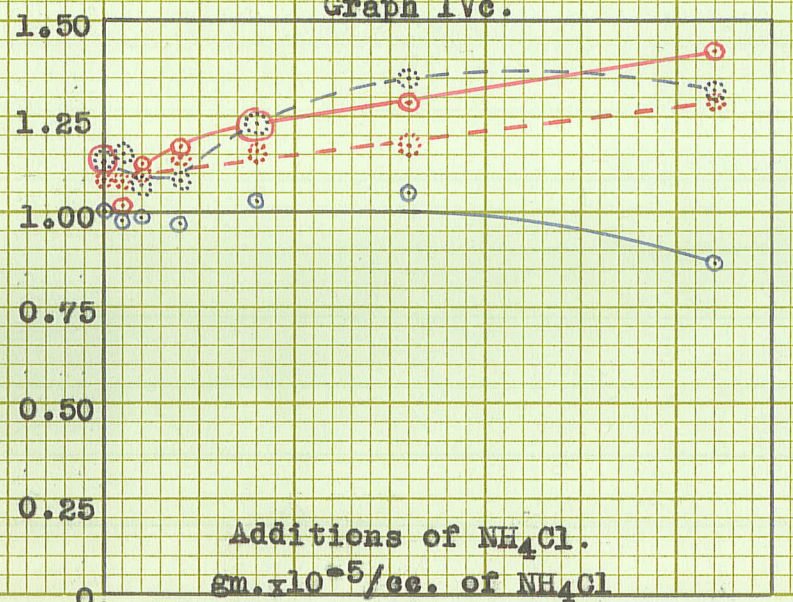


## Graphs IV.

Variations of the Intensity Ratio PbI 2833/MgI 2852, with Variations in the Extraneous Composition of Solutions Buffered with different Amounts of the same Substance

⊙—⊙ Unbuffered Solutions.

⊙ - - ⊙ Solutions buffered with $KNO_3$, 0.0064 gm. of K/cc. of solution.

⊙ - - ⊙ Solutions buffered with $KNO_3$, 0.0128 gm. of K/cc. of solution.

⊙—⊙ Solutions buffered with $KNO_3$, 0.0258 gm. of K/cc. of solution.

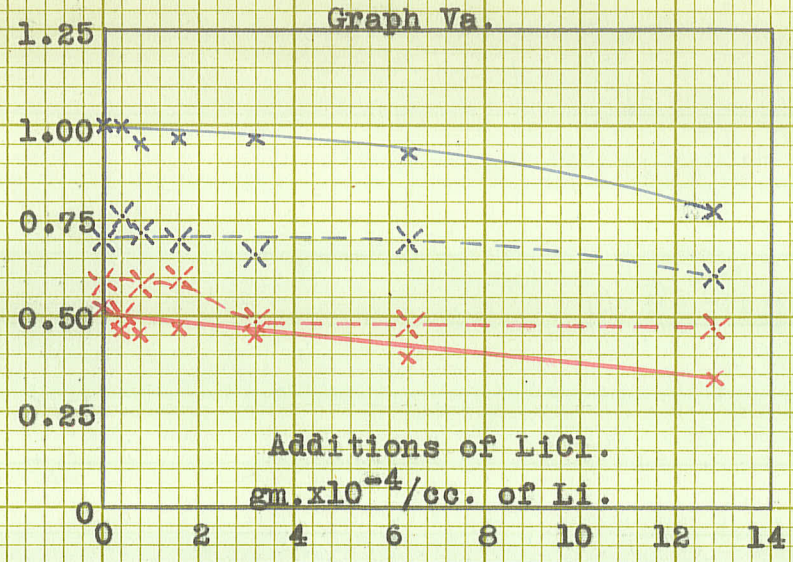


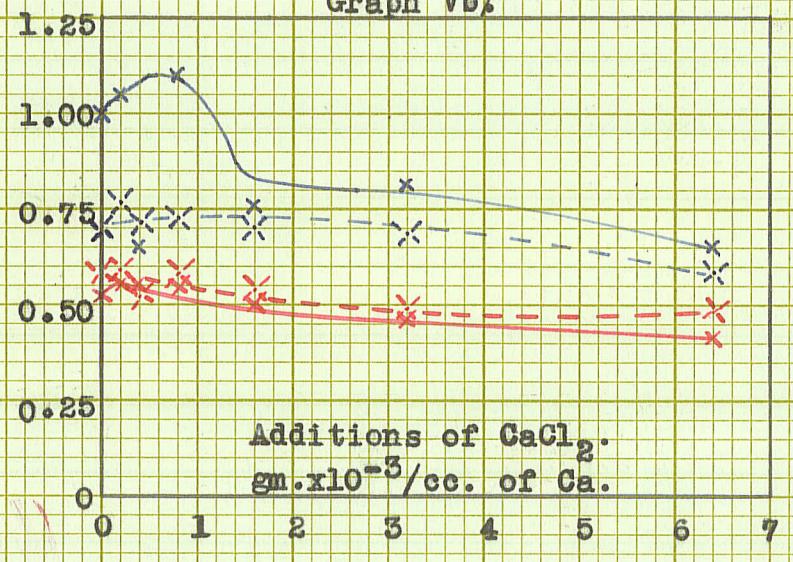


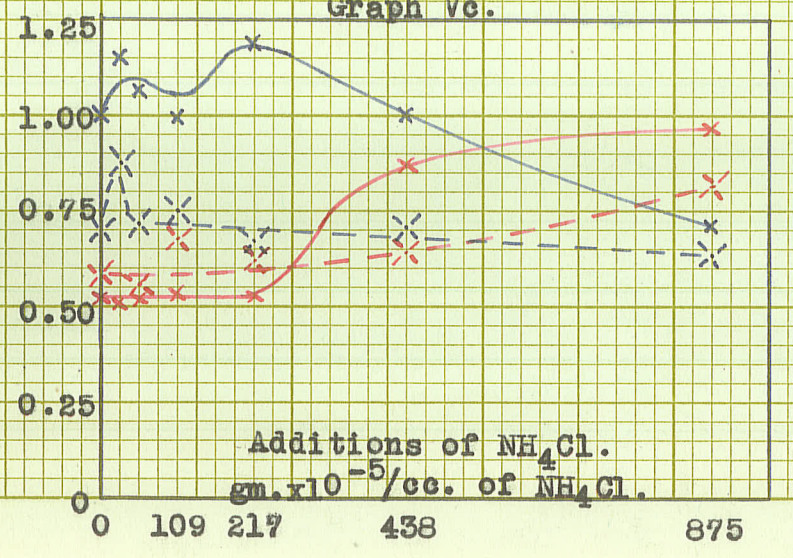


Graphs V.

Variations of the Intensity Ratio CdI 3261/MgI 2852, with variations in the extraneous Composition of Solutions Buffered with different amounts of the same Substance.

×——× Unbuffered Solutions.

×- - -× Solutions buffered with $KNO_3$, 0.0064 gm. of K/cc. of solution.

×- - -× Solutions buffered with $KNO_3$, 0.0128 gm. of K/cc. of solution.

×——× Solutions buffered with $KNO_3$, 0.0256 gm. of K/cc. of solution.

buffer used is a factor to be considered. As the concentration of ammonium chloride is increased, the cadmium to magnesium ratios show a marked decrease for the unbuffered samples; this decrease grows less when buffer is added to the samples, there being little change in the ratios for the two intermediate loads of buffer; finally, as the concentration of buffer is still further increased, the ratios show a marked increase as the concentration of ammonium chloride is increased.

It is clear from these results, that the use of a buffer in a sample, may or may not stabilize the intensity ratios of the lines of elements present in constant amounts in the samples, under changes in the extraneous composition of the samples. The effects produced depend on the elements whose intensity ratios are considered, and on the kind and amount of the buffer used.

The ratios plotted in the preceding graphs have dealt exclusively with the resonance lines of lead, cadmium, and magnesium. The intensity ratios of lines coming from higher levels within these atoms have also been studied (viz. PbI 2614/MgI 2780, CdI 3404/MgI 2780). The effects of extraneous composition variations on such ratios were similar, but, in general, more marked than the corresponding effects for the resonance lines of each pair of elements.

Effects of variations in extraneous composition on the inter spectra intensity ratios of lines emitted from different portions of the source.

The use of a condensing lens to focus an image of the spark on the spectrograph slit enabled the study of the effects of extraneous composition on the relative intensities of lines emitted from different portions on the axis of the spark. The Graphs VI record ratios obtained from unbuffered loads of standard solution, the intensity ratios PbI 2833/MgI 2852, PbI 2614/MgI 2780, CdI 3261/MgI 2852, and CdI 3404/MgI 2780 being plotted against additions of lithium chloride. The curves of Graph VIa are for light emitted from the axis of the spark near the plane electrode. The curves of Graph VIb are for emission from the axis near the pointed electrode, and the curves of Graph VIc for emission from the spark as a whole (i.e. no condensing lens was used).

Comparison of the Graphs VI shows that the changes in relative intensity with variations in the extraneous composition of the samples occur in different ways, in general, depending on whether light from only a portion of the spark is used, or whether light from the whole

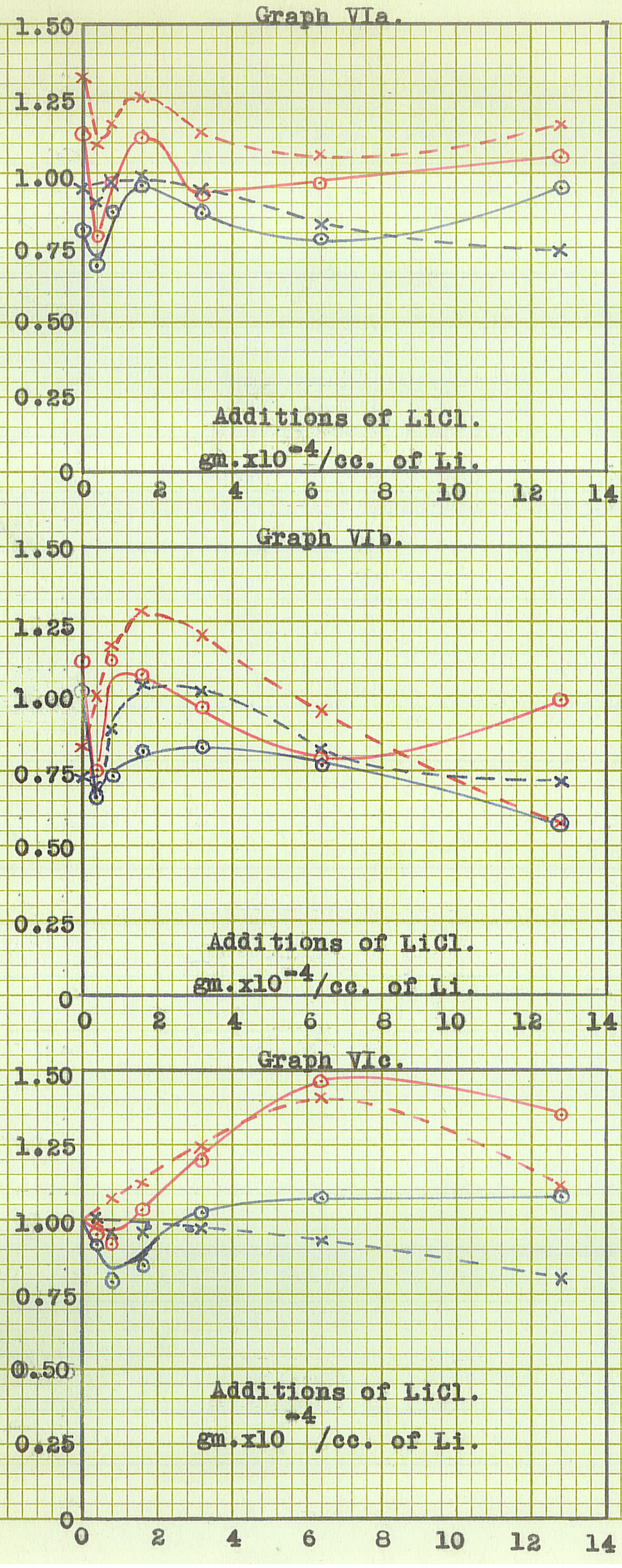


Graphs VI.

Effects of variations in extraneous composition on the inter spectra intensity ratios of lines emitted from different portions of the spark. Unbuffered Solutions.

VIa. Intensity ratios on axis of spark, near plane electrode.

VIb. Intensity ratios on axis of spark, near pointed electrode.

VIc. Intensity ratios from spark as a whole.

PbI 2833/MgI 2852.

CdI 3261/MgI 2852.

PbI 2614/MgI 2780.

CdI 3404/MgI 2780.

spark was admitted to the slit of the spectrograph. This was found to be true of all the extraneous additions used, for both buffered and unbuffered solutions.

Reproducibility of the ratios was not as good when a condensing lens was used as when no condensing lens was used. This is easily understood in view of the variations in the intensity ratios along the axis of the spark, and in view of an observed tendency in the spark to waver somewhat from side to side. It may be concluded that when a condensing lens is used, it is important for reproducibility, that light from the same portion of the source be admitted to the dispersing instrument at all times. This condition is very difficult to attain due to the fluctuations of the spark in space. Since a condensing lens may be used to advantage in many cases, where high sensitivity and high resolution are desired, it may be necessary to sacrifice reproducibility, and hence accuracy, to these other considerations.

# Intra Spectrum Ratios

Effects of variations in extraneous composition on the intra spectrum ratios of buffered and unbuffered samples.

In the Graphs VII and VIII, the intra spectrum ratios MgI 2780/MgI 2852, PbI 2614/PbI 3640, PbI 3640/PbI 2833, and CdI 3404/CdI 3261 are plotted against the extraneous additions. The curves of Graphs VII are for unbuffered solutions. The Graphs VIII illustrate the changes in the ratios with varying additions of lithium chloride, for solutions buffered with three different amounts of potassium nitrate, the amount of buffer being constant for the curves plotted in a given frame.

The Graphs VII show that there are changes in the intra spectrum intensity ratios as additions of extraneous material are made to unbuffered solutions. It may be noted that the cadmium to cadmium ratios are in general more stable under varying additions than the other ratios plotted. The magnesium to magnesium ratio 2780/2852 decreases with increasing amounts of all the additions.

The curves of Graphs VII are not indicative of any close relationship between the changes in the intra spectrum ratios and the corresponding inter spectra ratios

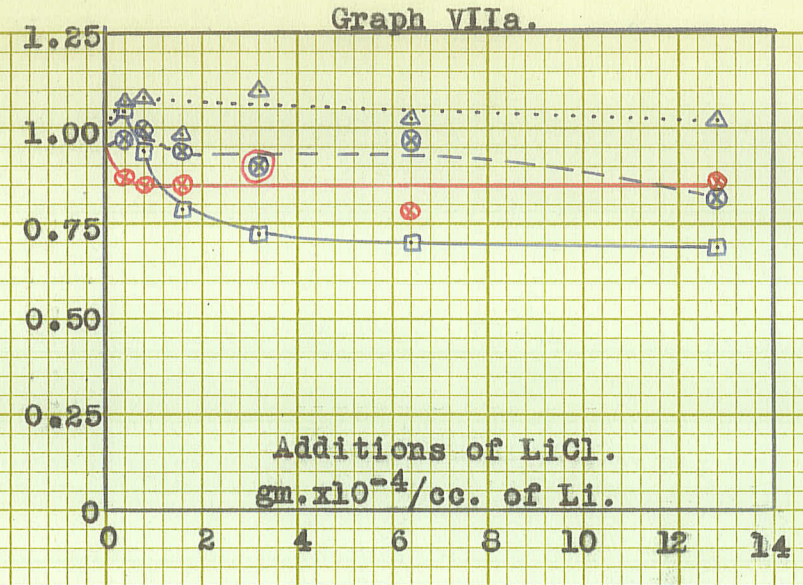


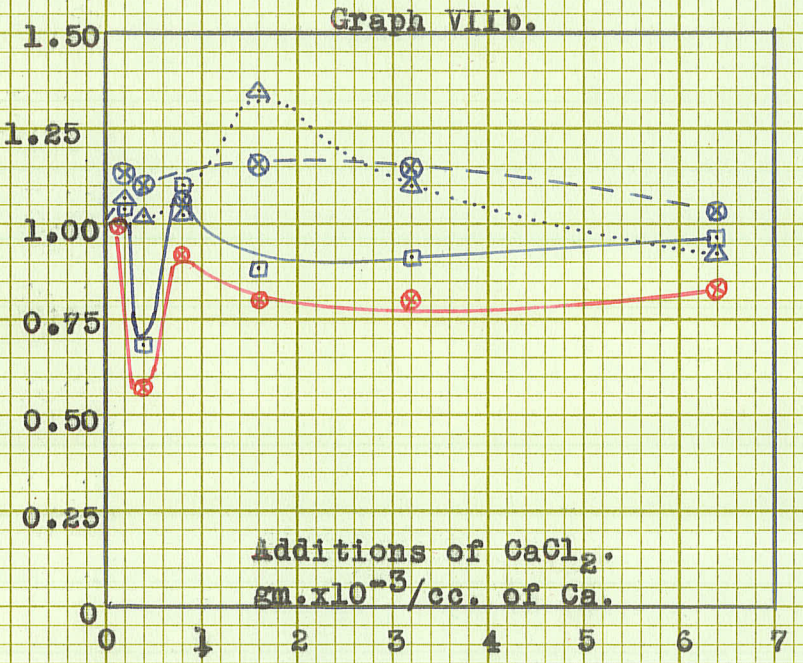


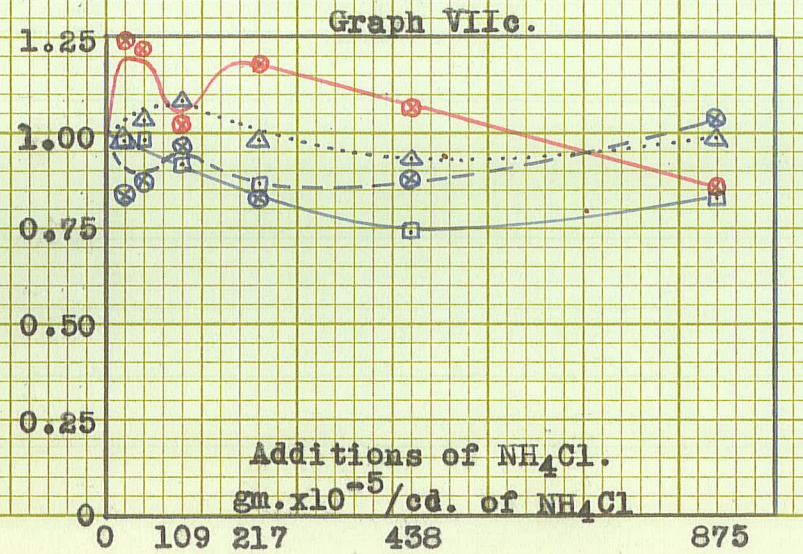


Graphs VII.

Effects of variations in extraneous composition on the intra spectrum intensity ratios of lines emitted from a-c spark. Unbuffered solutions.

MgI 2780/MgI 2852.

PbI 2614/PbI 3640.

PbI 3640/PbI 2833.

CdI 3404/CdI 3261.

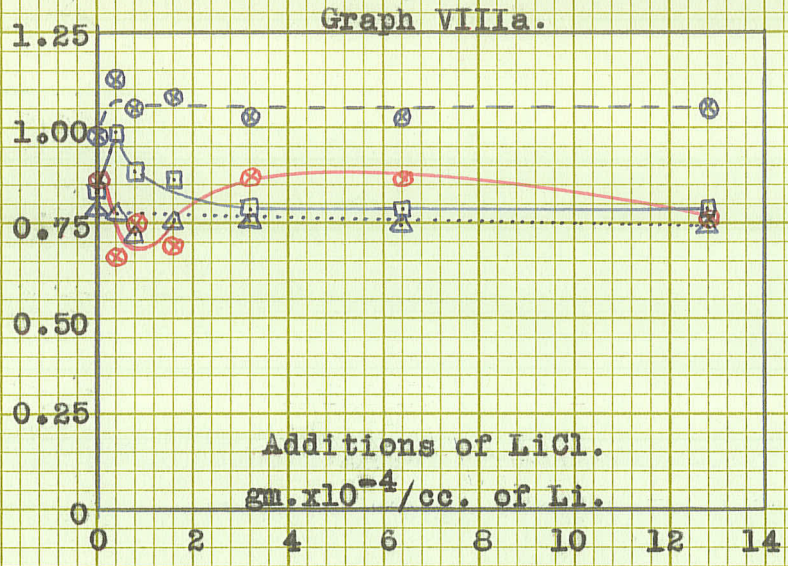


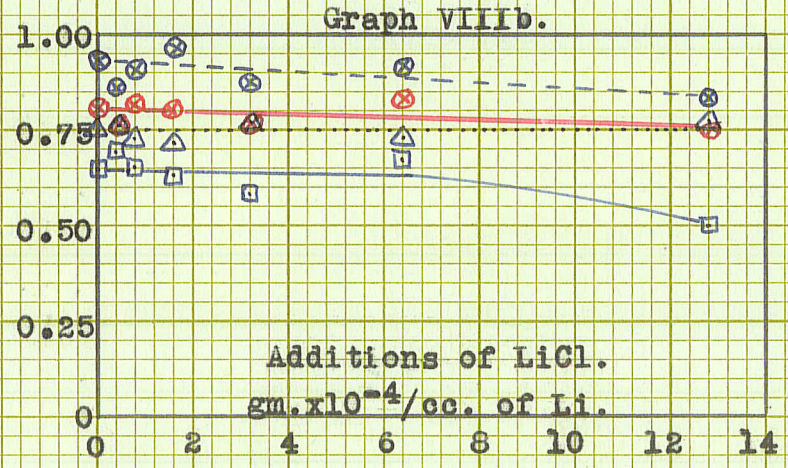


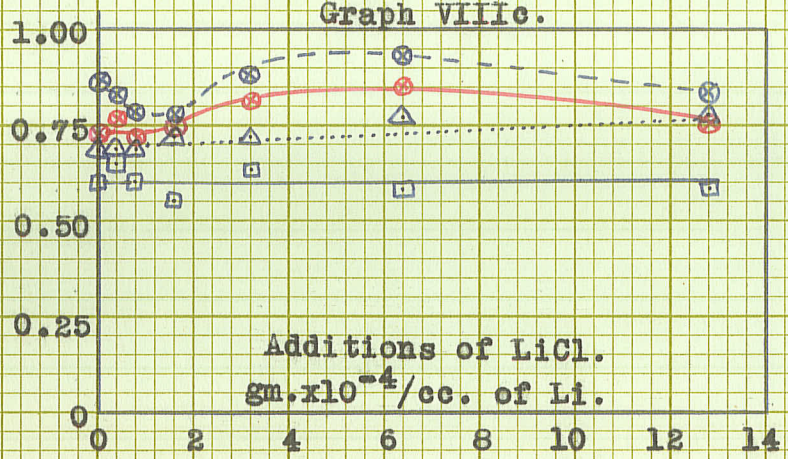


## Graphs VIII.

Effects of variations in extraneous composition on the intra spectrum intensity ratios of samples containing different amounts of buffer, in the form of $KNO_3$.

VIIIa. Solutions buffered with $KNO_3$, 0.0064 gm. of K/cc. of solution.

VIIIb. Solutions buffered with $KNO_3$, 0.0128 gm. of K/cc. of solution.

VIIIc. Solutions buffered with $KNO_3$, 0.0256 gm. of K/cc. of solution.

MgI 2780/MgI 2852.

PbI 2614/PbI 3640.

PbI 3640/PbI 2833.

CdI 3404/CdI 3261.

(cf. Graphs Ic, d, and e). The implications of this fact will be considered later.

Comparing the curves of Graphs VIII with those of Graph VIIa, it is apparent that the changes in the ratios with extraneous composition vary, depending on the amount of buffer present in the sample. The use of a buffer has a stabilizing effect on some of the ratios, and in general, increases the reproducibility of the ratios.

Effects of variations in extraneous composition on the intra spectrum intensity ratios of lines emitted from different portions of the spark.

The Graphs IX indicate the changes with extraneous composition of the intra spectrum intensity ratios of light emitted from different portions of the spark, namely, from two points on the axis of the spark one near each electrode and from the spark as a whole. These ratios correspond to the inter spectra ratios of the Graphs VI.

The Graphs IX show clearly that the behaviour of the ratios with changes in extraneous composition, may vary considerably, depending on the portion of the spark whose light emission is examined. Hence, the changes which take place in the discharge with variations in extraneous composition must be extremely complex. The significance of this will be considered later.

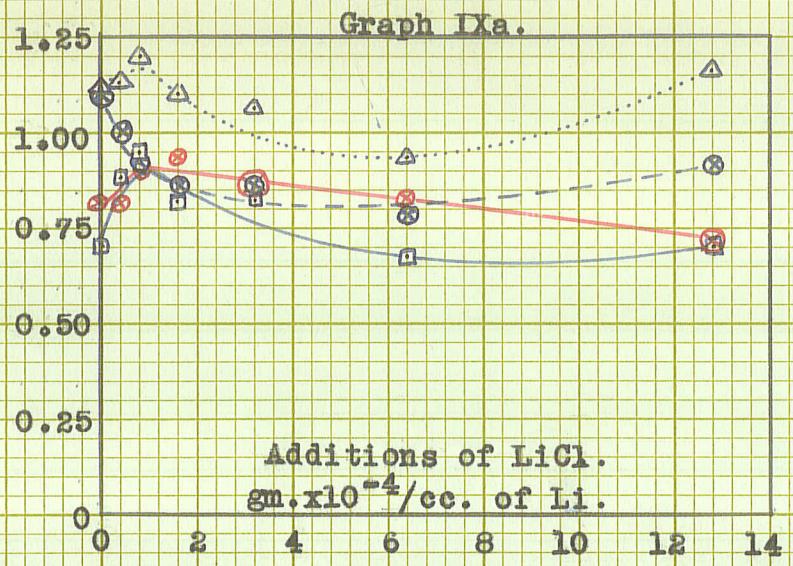


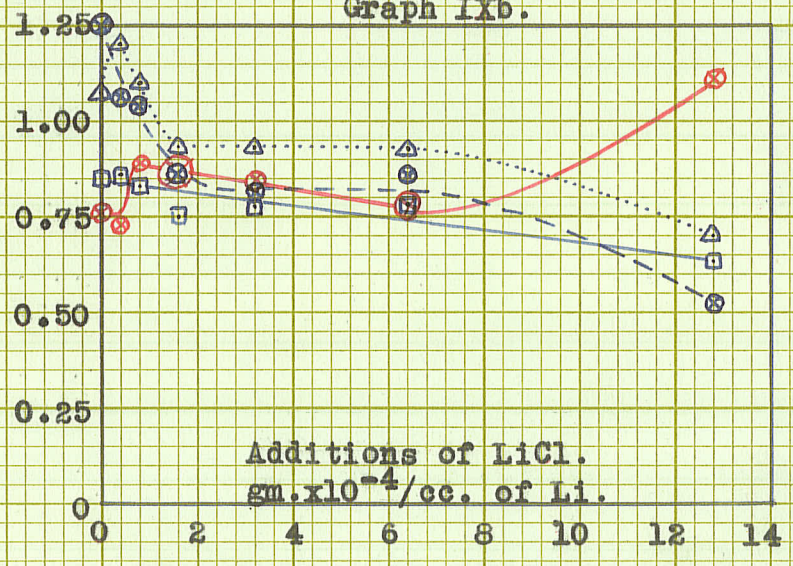


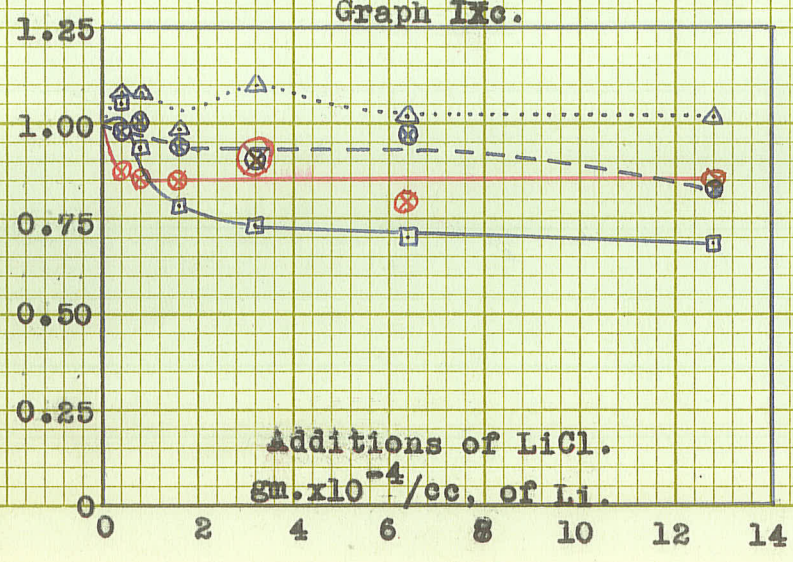


## Graphs IX.

Effects of variations in extraneous composition on the intra spectrum intensity ratios of lines emitted from different portions of the spark. Unbuffered Solutions.

IXa. Intensity ratios on axis of spark, near plane electrode.

IXb. Intensity ratios on axis of spark, near pointed electrode.

IXc. Intensity ratios from spark as a whole.

MgI 2780/MgI 2852.

PbI 2614/PbI 3640.

PbI 3640/PbI 2833.

CdI 3404/CdI 3261.

Effects of variations in extraneous composition on the intensity ratios of the ion to neutral spectra of magnesium. Increase in the intensity of the spectrum of the extraneous substance.

A very striking feature, common to all additions to the unbuffered sample was the marked decrease in the ratio of the ion to neutral lines of magnesium with increasing concentration of the extraneous material. This phenomenon was not observed for buffered solutions (cf. Graph XI.).

Some correlation between the decrease in the ion to neutral ratios and the increase in intensity of the extraneous material is clearly shown by the Graphs X. It is apparent that a gradual decrease in the ion to neutral ratios is associated with a gradual increase in the extraneous to magnesium ratios (cf. Graph Xa.), while a more rapid decrease in the ion to neutral magnesium ratios is associated with a more rapid increase in the extraneous to magnesium ratios (cf. Graph Xb.). For this reason, it is felt that this phenomenon can be explained qualitatively on the basis of Saha's theory of thermal ionization.[9]

9. Saha, M.N. Zeits. f. Physik, 6:40. 1921.

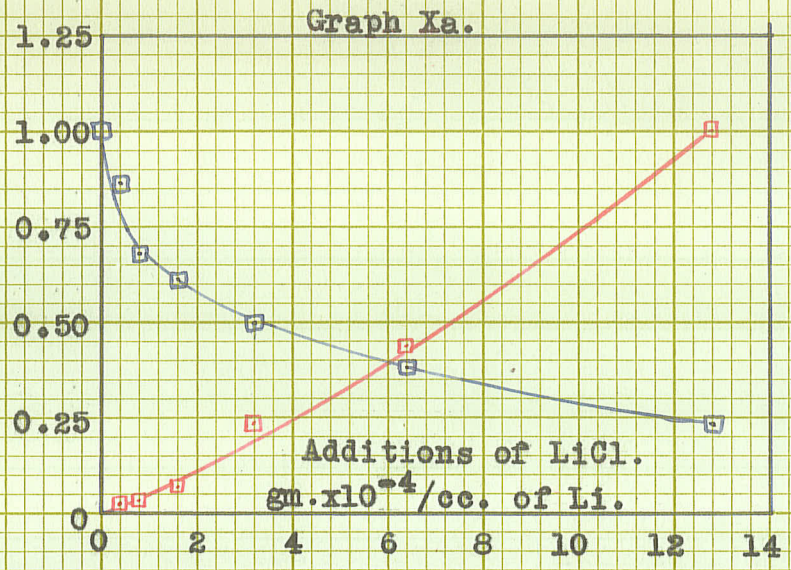


Graphs X.

Effects of variations in extraneous composition on the magnesium to neutral ratios and on the extraneous to magnesium ratios of unbuffered solutio

MgII 2937/MgI 2780.

Xa. LiI 4603/MgI 2780

Xb. CaI 3159/MgI 2780.

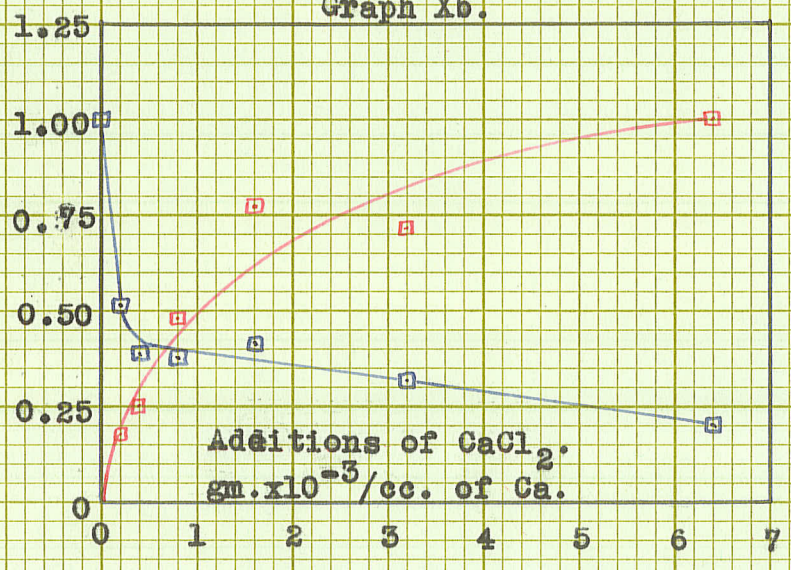


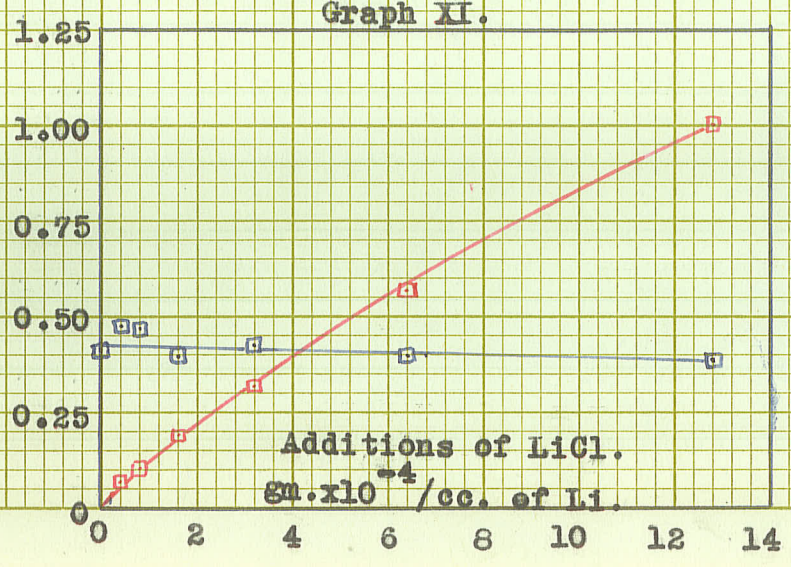


Graph XI.

Effects of variations in extraneous composition on the magnesium to neutral ratios and on the extraneous to magnesium ratios of solutions buffered with $KNO_3$, 0.0128 gm. of K/cc. of solution.

MgII 2937/MgI 2780.

LiI 4603/MgI 2780.

Qualitatively, this theory may be interpreted to mean that the number of ions of a given element present in the discharge will decrease, as the number of ions of another element increases. Since the number of ions of the extraneous element present in the discharge will increase with the amount of this element in the discharge, it is clear that Saha's theory will explain qualitatively the changes in the ion to neutral spectra of magnesium with variations in the extraneous composition of unbuffered solutions.

Further, the constancy of the ratios of the ion to neutral spectra of magnesium with variation in the extraneous composition of buffered solutions can be explained on the basis of this theory. One would not expect relatively small additions to a load heavily buffered with potassium nitrate to reduce appreciably the number of ions of a given substance already present in the discharge, owing to the large number of ions which such a buffer would contribute to the discharge.

# Discussion.

Thermal effects in the source.

The investigations of Langstroth and McRae[10] have indicated that the excitation in a condensed spark discharge produced by circuits having a fairly long oscillation period ($10^{-4}$ seconds) may be considered thermal in character, just as in the freely burning arc.[11]

A close approximation to the oscillation period of a spark circuit, such as used in these experiments, may be obtained[12, 13] by the use of the relation

$$T = \frac{2\pi}{\sqrt{\frac{1}{LC} - \frac{R^2}{4L^2}}} \qquad \ldots\ldots\ldots\ldots\ldots\ldots\ldots\ldots (1)$$

where T, R, L, and C denote respectively, the period, resistance, inductance, and capacity of the circuit.

For the circuit used in these experiments, L was 120 microhenries, C was 0.03 microfarads, and R may be assumed to be of the order of 3 ohms. Substituting these values in (1), the period of the circuit turns out to be approximately $8 \times 10^{-6}$ seconds.

10. Langstroth, G.O., and McRae, D.R., Can. J. Research, A,16:17-27. 1938.

11. Mannkoppf, R. Zeits. f. Physik, 86:161-184. 1933.

12. Milner, S.R., Phil. Trans., A, 209:71-88. 1909.

13. Royds, T. Phil. Trans., A,208:333-347. 1908.

This period is somewhat short, but the lack of air lines in the spectra produced shows that the light emitted by the spark comes mainly from the arc-like phase (see Appendix III). Since the excitation in the freely burning arc is thermal in character, it may be assumed that the excitation in the spark source used in these experiments is also predominantly thermal.[10]

Mannkoppf[11] has stated that, in the arc, the only influence of an extraneous element is a change in temperature. If this statement can be applied to the condensed a-c spark, it should be possible to correct for the changes in the ratios due to variations in the extraneous composition, since the mode of variation of line intensity with temperature is known.

Assuming predominantly thermal excitation in the spark, and hence, a Maxwell-Boltzmann distribution of the atoms among the energy levels, a temperature change, $\Delta T$, can be measured by use of the relation

$$\Delta T = - \frac{k\, T^2 \Delta I_{12}}{\Delta E\, I_{12}} \qquad \text{.....(2)}$$

which is easily derived from

$$I_{12} = A P_{12}\, e^{- \Delta E/kT} \qquad \text{.....(3)}$$

where A is a constant depending on the frequencies and populations of the initial and final levels, and

where $I_{12}$ is the intensity ratio of a line coming from a higher level within the atom to a line coming from a lower level, the ratio of the transition probabilities for the two lines being $P_{12}$; $\Delta E$ is the energy difference between the initial levels of the lines; k is the Boltzmann constant; T is the absolute temperature; and $\Delta T$ is the temperature change corresponding to a change of $\Delta I_{12}$ in the intensity ratio of the two lines.

Equation (2) permitted the calculation of temperature changes in the spark, from the changes $\Delta I_{12}$ in the intensity ratio $I_{12}$ of two lines with different initial energy levels within an element. k has a value of $1.37 \times 10^{-16}$ ergs per degree absolute. $\Delta E$ can be determined from the energy level diagram (cf. fig. 2.) of the element whose lines are considered.[14, 15] An approximate value of T was determined from experiments on the tin ratios 3262/3175, and 3262/3034 which have been calibrated for temperature against the cyanogen bands.[10] The 'temperature' of the spark was found to be about 7000°A.

14. Bacher, R.F., and Goudsmit, S., Atomic energy states. 1st ed. McGraw-Hill Book Co., New York. 1932.

15. Grotrian, W. Graphische Darstellung der Spektren. 1st ed. Springer, Berlin. 1928.

If the effects of variations in the extraneous composition are due primarily to temperature changes in the source, then the intra spectrum ratios of two lines having respectively high and low initial levels, would be expected to change in the same general way for each element of the standard sample (cf. equation 2), with additions of extraneous substance. An examination of the Graphs VII and IX shows that this is not in general the case, for the data of these experiments. Further, calculation shows that the temperature change, required to reduce the intensity of the ion to neutral magnesium ratio 2937/2780 in the manner evidenced in the Graphs X is less than 100°A; this effect has been explained on the basis of Saha's thermal ionization theory. The constancy of the ratio 2937/2780 in the case of buffered solutions limits temperature changes in the spark to the order of 10°A. In any case, a temperature change of 100°A. would not produce measurable change in the intra spectrum ratios of magnesium, cadmium and lead, which have been studied during this experimentation. Hence, it must be concluded that, in the condensed a-c spark, the changes with extraneous composition in the intensity ratios of lines emitted by the spark cannot be explained on the basis of temperature changes in the source.

For this reason, the method of correction of the intensity ratios for the effects of extraneous composition, proposed by Levy[16], and based on the assumption that the effects were due entirely to temperature changes in the source, has not been found applicable to the data obtained during these experiments.

16. Levy, S. J. of Applied Physics, 11:480-487. 1940.

Uneven separation of load materials on the electrodes.

All loads, with the exception of those buffered with sodium potassium tartrate dried somewhat unevenly on the electrodes, leaving a rough surface, and a ring of material around the edges. The varying solubilities of the materials in the loads (0.0073 gm. of lead per cc.; 0.144 gm. of magnesium per cc.; and 0.86 gm. of cadmium per cc.) would undoubtedly contribute to the uneven distribution of substances on the electrodes. Lead, with the least solubility would be deposited first, and relatively more lead than magnesium or cadmium would be expected in the ring of material around the edges of the electrode, where the rate of evaporation is greatest, due to the greater curvature of the surface of the solution.

It has been noted before that the inter spectrum ratios of the resonance lines, and of lines with high initial levels, of two of the standard elements used in these experiments, change in somewhat the same general manner with variations in extraneous composition; with the possible exception of the ratios derived from data where the loads were buffered with sodium potassium tartrate. Since loads which dried to all outward appearances uniformly did not show these general changes, while those which dried

did, it is clear that these general changes in the spectrum of one element relative to that of another can be most easily explained on the basis of changes in the distribution of material on the electrodes.

However, the use of sodium potassium tartrate as a buffer did not stabilize the inter spectra ratios to the effects of variations in extraneous composition, as well as did potassium nitrate (cf. Graphs II and III). Hence, the changes in the inter spectra ratios observed with variations in extraneous composition of the sample, can be only partially due to the uneven distribution of material on the electrodes.

Atomic Interactions in the Spark.

The mechanisms of release of material from the electrodes and the mechanisms of excitation of the atoms within the discharge must be of a very complex nature.[10] The excitation of the atoms doubtless involves collisional processes, and hence must depend on a number of factors, such as the number of elastic and inelastic collisions, the collisional cross section, ease of ionisation and masses of the particles.

Evidence of the complexity of the situation arises in the present experiments, in the form of an anomolous behaviour of the lead to lead ration 3640/2833 (cf. Graphs VII, VIII and IX). These two lines have the same initial level (cf. fig. 2), and hence their ratio would not be expected to change with temperature (cf. equation 2). The ratio might change somewhat with variation in the amount of lead within the spark gap, due to changes in the self absorption effects in the cooler layer of gases which surrounds the spark. However, for solutions containing a constant amount of buffer, the intensity of the lead spectrum did not vary appreciably, as indicated by the small changes in the density of silver deposit on the photographic plates for a constant exposure time. Hence, it is unlikely that the changes in this ratio can be explained on the basis of changes in self absorption

It must be concluded, therefore, from these considerations, and from the evidence of the complex changes which occur in the relative concentrations and energy distributions of the elements in different portions of the spark (cf. Graphs VI and IX), that a complete explanation of the changes produced by variations in the extraneous composition of the sample will be possible only when detailed knowledge is available of the factors which vary the mechanisms involved in the release of material from the electrode, and the transport and excitation of the constituent atoms in the spark gap.

# Conclusions.

The following general conclusions may be drawn concerning the effects of extraneous materials on the relative intensities of spectral lines, under the conditions of these experiments.

(1) Variation in the extraneous composition of a sample may cause changes in the relative intensities of a pair of spectral lines, not only for lines emitted by two different elements, but also for lines emitted by the same element.

(2) These changes in intensity ratios are not the result of 'temperature' changes within the discharge, but may be due partly to variations in the distribution of the load on the electrodes, partly to variations in the mechanism responsible for the release of material from the electrodes, and partly to variations in the phenomena of diffusion and excitation in the discharge column.

(3) The changes in the ratios with variation in the extraneous composition depend on the nature and amount of the spectroscopic buffer used.

(4) The use of a buffer does not, in many cases result in a constancy of the ratios with variation in the extraneous composition of the sample, but does aid in the reproducibility under any given set of conditions.

(5) The effects of the variations in the extraneous composition on the intensity ratios depends on the portion of the source from which light is examined; i.e. depends on the use or otherwise of a condensing lens. The use of a condensing lens is accompanied by a decreased reproducibility of the ratios under any given set of conditions.

(6) For unbuffered solutions the relative intensity of the ion spectrum of magnesium to the neutral atom spectrum of magnesium decreases very markedly with increasing extraneous additions, the greater rate of decrease in the one corresponding to a greater rate of increase in the other.

Part B.

# A Direct Reading Photoelectric Microphotometer.

In collaboration with
Dr. G. O. Langstroth, and
Mr. W. W. Brown, B.Sc.

## Introduction

In quantitative spectrographic analysis, a microphotometer is an instrument used to measure the transmission of a silver deposit on a photographic plate. In order to do this (cf. fig. a) light from a source S is focussed by means of a lens C on the portion of the plate P at which the transmission is to be measured.

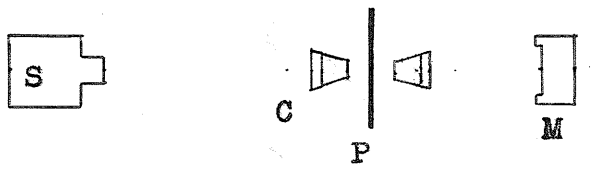


fig. a.

The transmitted light energy is then measured by a suitable device M, such as a photovoltaic cell and galvanometer circuit. The ratio of the light energies transmitted when the silvered portion of the plate is in the beam, and when 'clear plate' is in the beam is called the 'transmission' of the silvered portion of the plate.

The following procedure is involved in the use of a microphotometer to determine the relative intensity of two lines, which have been recorded in a spectrum on a photographic plate:

(i) calibration marks are put on the plate (cf. Plate III), consisting of an exposure during which a series of known intensities of light of a wavelength comparable to the wavelengths of the lines whose intensity ratio is to be measured. It is not necessary to know the absolute intensities

used to obtain the calibration marks, but only their relative values, as later procedure involves the taking of the ratio of two intensities.

(ii) the transmissions of the series of marks are measured on the microphotometer.

(iii) a calibration curve for the plate is prepared (cf. Appendix V) consisting of the transmissions of the calibrations plotted on a linear scale against light intensities on a logarithmic scale.

(iv) The transmissions of the two lines whose intensity ratio is desired are measured on the microphotometer, and the corresponding intensities are read off the calibration curve prepared in (iii).

(v) the ratio of the intensities of the lines is then calculated.

This section of the thesis describes a direct reading photoelectric microphotometer which has been constructed at a relatively low cost. The instrument has the advantages of speed and convenience of operation with minimum fatigue to the operator. These qualities are attained through the arrangement of the optical system and controls, the design of the plate movement, and the method of making the observations.

## General Design.

The general features of the design may be seen from Plate IV and fig. 3. The optical train is a modification of that used in most microphotometers. It is so arranged that the photographic plate, the observation screen containing the slit which admits light to the photocell, and the galvanometer scale are grouped together, one above the other, in approximately the same plane with respect to the operator's eye. This grouping of the parts which must be under constant observation has been made with a view to minimizing the fatigue inherent in the continuous use of a microphotometer over an appreciable period of time. With the same aim, the various controls have been grouped in convenient positions as indicated in the illustrations.

The galvanometer is situated below and behind the instrument. Light from its mirror is focussed on a ground glass scale set into the top of an inclined drawing board and contiguous with a 9 by 10 inch glass plate also set into the board. A sheet of semi-logarithmic graph paper placed on the plate with the linear scale lying along the galvanometer scale is illuminated from the back with red light. This arrangement provides excellent illumination for observing

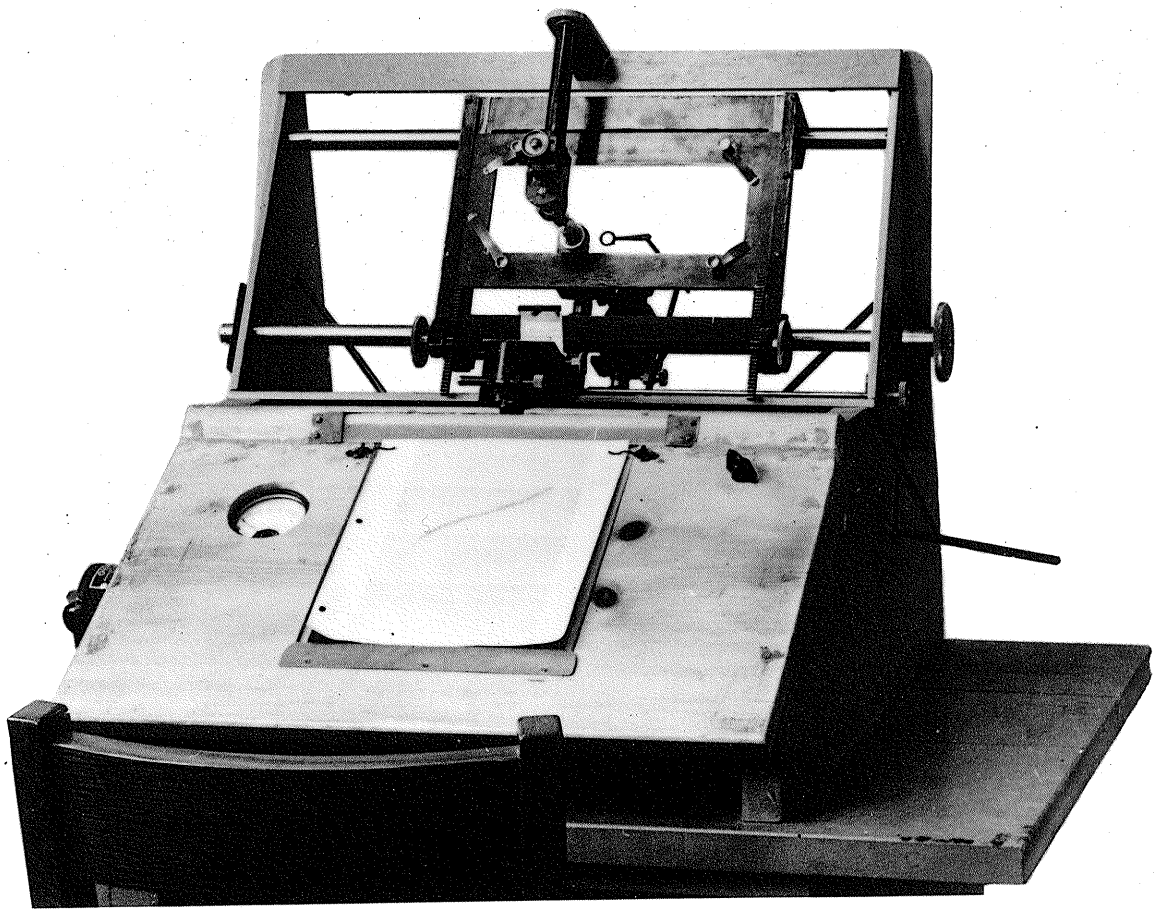

Plate IV.

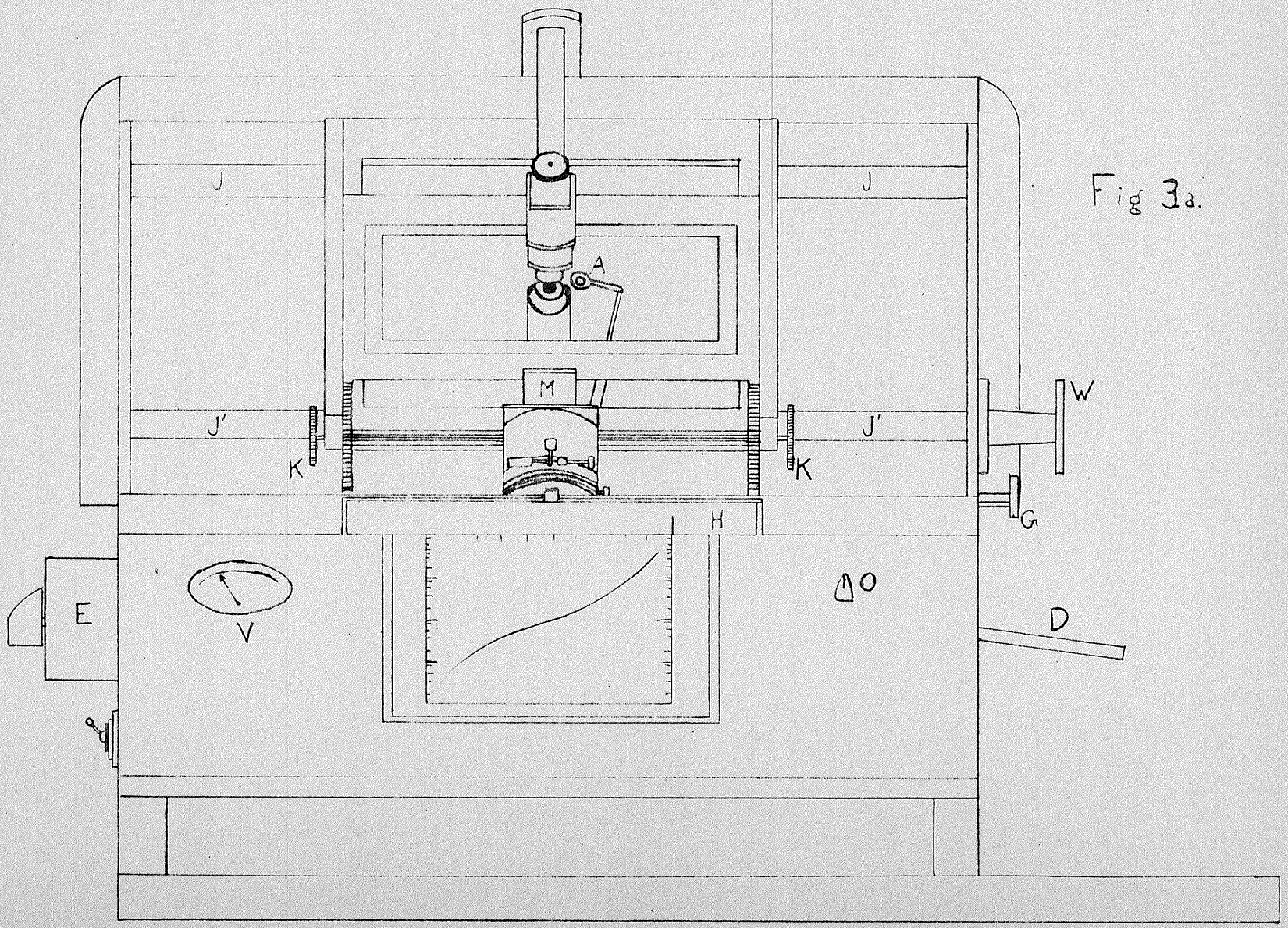


Fig 3a.

Key to Symbols used in figs. 3. and 4.

S. Automobile lamp.

L. Adjustable slit and lens unit.

A. Auxiliary lens.

C. Condensing objective.

F. Focussing objective.

P. Reflecting prism.

B. Observation screen with slit, mounted on photocell housing.

M. Observation mirror.

H. Galvanometer scale.

V. Voltmeter connected across S.

W. Fine micrometer adjustment for horizontal plate motion.

K. Rack and pinion adjustment for vertical plate motion.

G. Micrometer adjustment for C.

R. Micrometer adjustment for F.

D. Lever adjustment for A.

O. Adjustment for series resistance in galvanometer circuit.

E. Adjustment for lamp current.

The adjustments for cross and vertical movements of the optical parts are not lettered.

Fig. 3b.

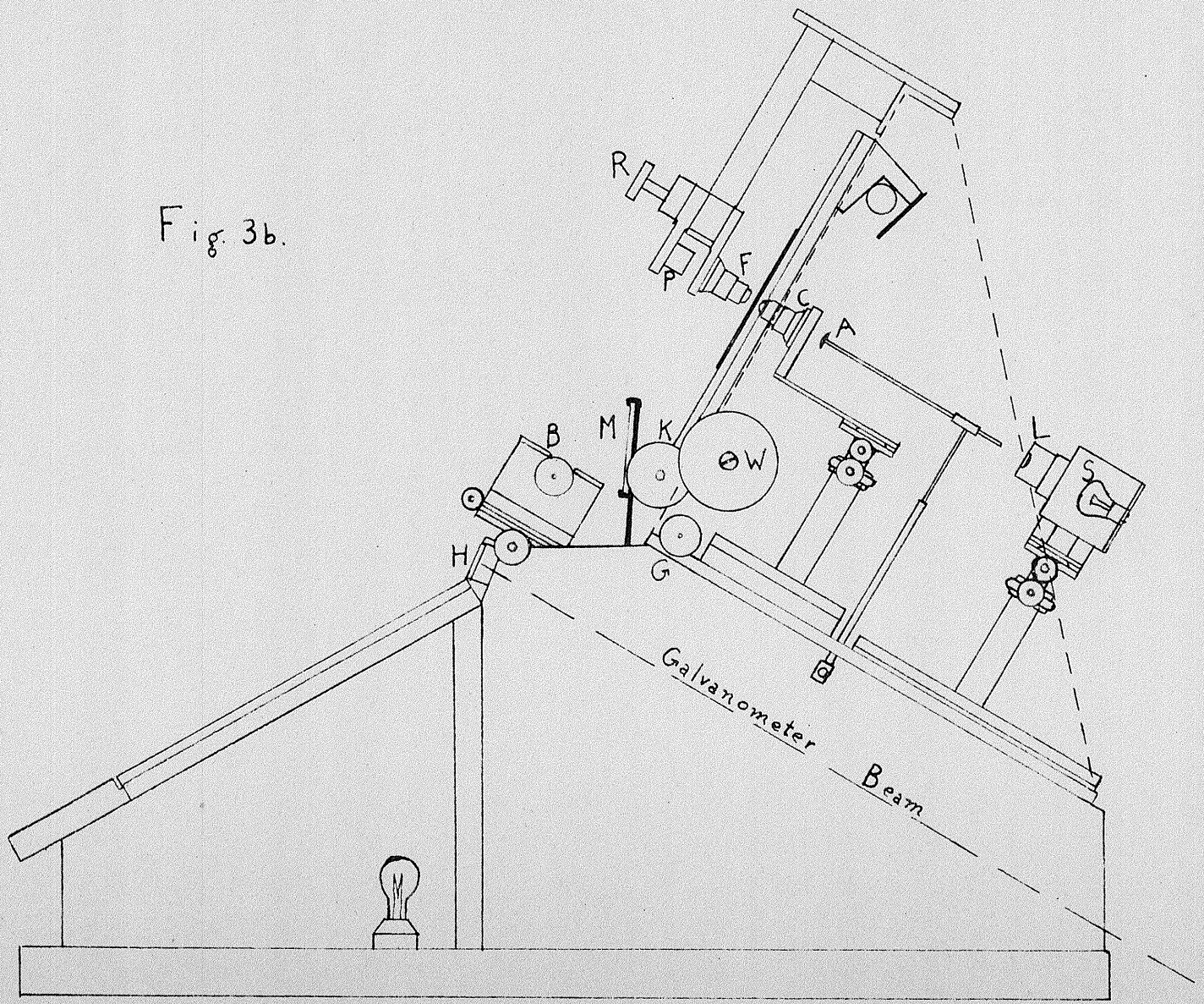

the graph coordinates, and minimizes the amount of scattered light in the microphotometer room. As will appear later, determination of relative intensities is possible without reading off numerical values for the galvanometer deflections and calculating the transmission value for each spectral line.

The plate holder is of sufficient size to permit the investigation of all parts of a standard 4 by 10 inch plate without readjustment in the holder. It is mounted on friction bearings which facilitate rapid rough adjustment lengthwise, combined with a micrometer adjustment for accurate setting on the desired spectral line. Further details are given later.

## The Mounting.

All parts of the optical system including the photocell are mounted on a framework of 5/16 inch boiler plate. Three inch channel iron and 1½ inch angle irons screwed respectively to the base and side plates ensure the necessary rigidity. The angle iron extending across the top of the frame work is reinforced with 1½ inch pipe. The framework is securely fastened to a cabinet of 1¼ inch maple.

## The Optical System.

The light source consists of a 6 volt 32 c.p. automobile lamp operated from a storage battery. The current through it is controlled by a 1 ohm "Ohmite" variable resistance; the potential drop across it is indicated by the voltmeter V (fig. 3.). The lamp housing carries a slit behind which is fixed an f:3.5, 3.5 cm. focal length lens. This unit is adjusted to form an image of the lamp filament approximately in the plane of the condensing objective. The condensing objective forms an image of the slit on the emulsion of the photographic plate, which in turn is focussed by the focussing objective on a white screen containing an adjustable photocell slit. Magnifications of 0.1 and 10 respectively are used. Both objectives are achromats of 16 mm. equivalent focal length and 0.25 numerical aperture. The photometer beam is directed to the observation screen by a fixed reflecting prism mounted about 3 cm. behind the focussing objective. The image on the screen may be conveniently observed by the operator in the plane mirror M.

Micrometer screws are provided for the axial adjustment of the objectives. Each optical part, with the exception of the focussing objective unit has cross and

vertical movements, and the observation screen has cross and rotational movements. Adjustment of the reflecting prism is made by means of three grub screws. All controls have been placed with a view to matimum convenience in operation.

An auxiliary lens A is provided. It may be swung into the photometer beam by means of the lever shown in the illustration. It permits observation of an appreciable range of the spectrum on the screen, and is used in the usual manner to obtain critical focus for the objective F.

## The Photocell Circuit.

A Weston Photronic cell is used as a detecting unit. It is connected in series with a 2000 ohm variable resistance and a Leeds and Northrup galvanometer (sensitivity $3 \times 10^{-9}$ amps./mm., period 2.6 seconds). Under ordinary conditions the changes made in the circuit resistance during operation are not sufficiently great to detectably affect the critical damping of the instrument.

## The Plate Holder and Plate Movement.

The metal plate holder which accomodates a 4 by 10 inch plate is fitted in ways attached to a larger rectangular frame. Vertical plate motion is accomplished by means of a rack and pinion at each side of the plate holder. The frame is hung from the upper bearing rod J (fig. 3.) by means of right angle bronze bearings, and is held against the outer surface of the lower rod by friction bearings (fig. 4a.). The lower rod may be moved endwise by means of a micrometer screw operated by a three inch wheel B (fig. 4b.). This arrangement allows rapid manual movement of the plate holder endwise, and at the same time makes provision for fine adjustment of the motion by means of the micrometer screw.

It is essential that the emulsion of the photographic plate should remain in the focal plane of the objectives over the entire range of the plate motion. This condition was fulfilled by the following procedure. (a) The bearing rods of $\frac{3}{4}$ inch cold rolled steel shafting were adjusted accurately parallel. (b) The movable bearing rod was keyed to prevent rotational motion, thus eliminating the possibility that some eccentricity in the rod might throw the emulsion out of the focal plane of the objectives.

Fig. 4a.

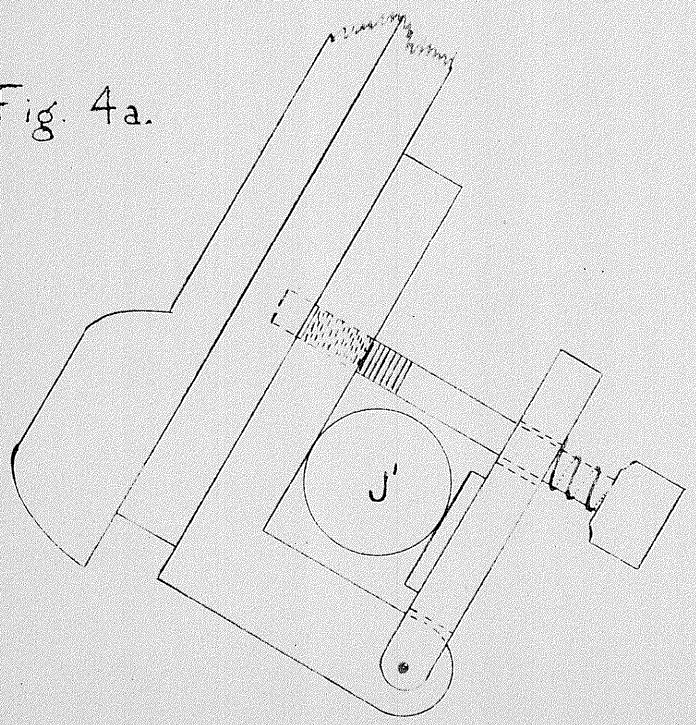


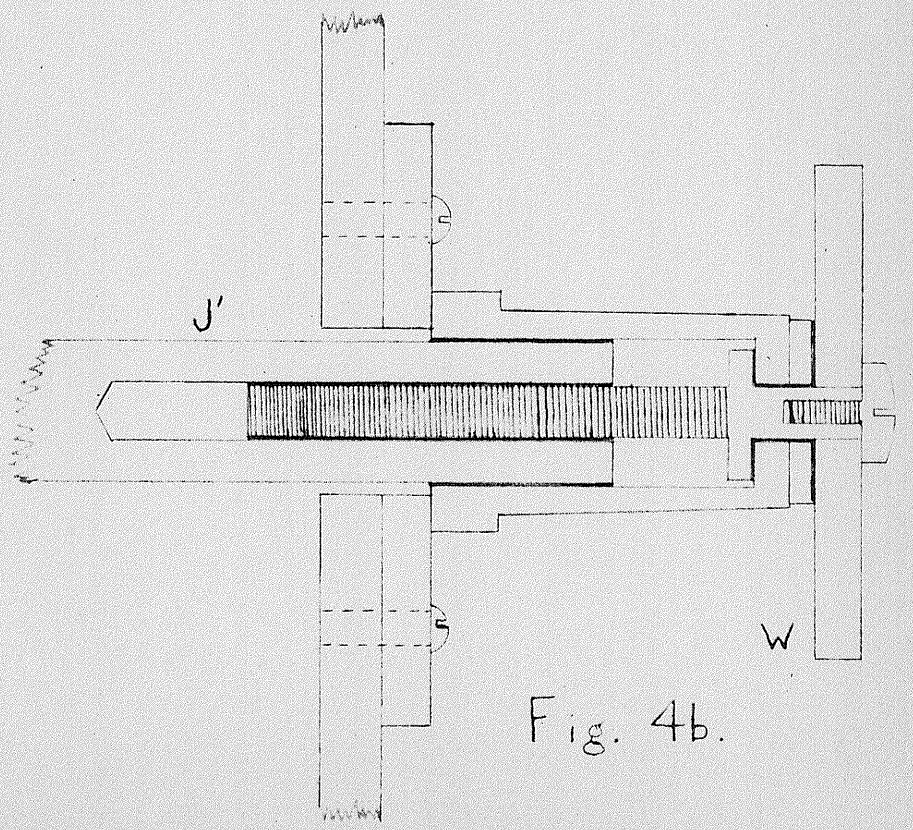


Fig. 4b.

(c) The bearings, and also the surface of the plate holder, were fitted by trial, using the critical focus of the emulsion on the observation screen as the criterion to be satisfied.

## Method of Making Observations.

The method used in determining relative intensities of spectral lines is a modification of that previously described by Langstroth and McRae.[17] As previously stated, a sheet of semi-logarithmic graph paper is placed with the linear scale lying along the galvanometer scale. It is adjusted so that the coordinate zero coincides with the galvanometer zero. The 'clear plate' deflection is adjusted to read 1.0 (10 large scale divisions) by means of the series resistance (fig. 1.). On introduction of a spectral line into the photometer beam, the deflection as read from the coordinate scale therefore represents the transmission value for the line. In plotting the calibration curve for the plate, the calibration marks are introduced successively into the beam; a point is plotted opposite each position of the galvanometer spot at the appropriate intensity value on the logarithmic scale. On subsequent introduction of a

17. Langstroth, G.O., and McRae, D.R., J. Opt. Soc. of America, 28:440.

spectral line into the beam, the relative intensity is read off directly from the curve, as that value on the logarithmic scale corresponding to the point on the calibration curve opposite the position of the galvanometer spot on the linear scale. This procedure obviates the reading of numerical values for the galvanometer deflections and the calculation of transmission ratios.

## Remarks.

The microphotometer described in this article has been in constant use for the past six months, and has been found to be time saving and convenient. In addition, the method of making the observations goes far toward the avoidance of arithmetical mistakes which sometimes occur when galvanometer deflections are recorded and transmission values calculated. The precision of the measurements is comparable with that of other direct reading instruments; viz. 2% maximum error for lines of moderate density.

Constant use has suggested that the instrument might be improved at a reasonable cost by substitution of a shorter period galvanometer. Furthermore, the micrometer wheel B controlling the plate motion might be placed on the left hand side of the instrument with some advantage.

Part C.

# An Experimental Investigation into the use of Collimated Light Beams in Spectrophotometry.

In collaboration with

Mr. W. W. Brown, B. Sc.

## Theoretical Introduction

On the basis of the Lambert-Beer law, the relation between the transmission $\tau_\lambda$ of light of wavelength $\lambda$, absorption coefficient $\mu_\lambda$, and length of path t in the absorption cell is

$$\tau_\lambda = e^{-\mu_\lambda t}$$

If the depth of the cell is $l$, and all the rays of light pass through the cell perpendicular to its faces, then

$$\tau_\lambda = e^{-\mu_\lambda l}$$

However, in the commonly used spectrophotometric system, consisting of line source of light of finite dimensions (e.g. a slit), 'collimating' lens, and absorption cell indicated in fig. b, very few of the light rays actually traverse the cell parallel to the optic axis of the system. Hence, the measured average transmission of the solution in the cell is given by

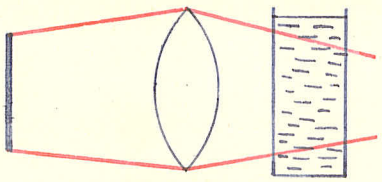

fig. b.

$$T_\lambda = \frac{\int_t e^{-\mu_\lambda t}\, dt}{\int_t dt}$$

Evaluating this integral, Langstroth obtained the relation (a second approximation)[18]

$$T_\lambda = e^{-d_\lambda}(1 - Kd_\lambda) \quad \ldots\ldots\ldots\ldots\ldots\ldots\ldots(4)$$

where

$$K = \frac{1}{2n^2p^2}\left[\frac{H^2}{3} + \frac{(p-f)^2(R_2^2 + R_1^2)}{2f^2}\right] \quad \ldots.(4a)$$

The symbols $d_\lambda$ ($d_\lambda = \mu_\lambda \ell$) and n denote respectively the optical density and refractive index of the solution, p represents the slit-to-lens distance, 2H the length of the slit, and f and $R_2$ the focal length and radius of the collimating lens. $R_1$ denotes the radius of an opaque disc centrally placed on the collimating lens. Equation (4) is simply the Lambert-Beer law with a correction factor. It is the magnitude of the changes in this correction factor with variation in the slit-to-lens distance, that is dealt with in the present research.

The correction factor does not reduce to unity when the source is placed at the principal focus of the lens (cf. equation 4a). However, calculation shows that even in extreme cases of high absorption, long slit and fast lens, the factor rarely introduces an error of more than 3% in the true transmission of the solution, by

18. Langstroth, G.O., J. Optical Soc. Am., 29:381-386. 1939.

taking the measured transmission as the true value.

So far, only the case when monochromatic light is involved has been considered. For a wavelength band of finite width, the effective transmission T is given by the ratio of the transmitted energy to the incident energy, each being summed over the band. That is

$$T = \frac{\sum_\lambda T_\lambda \, \phi(\lambda)}{\sum_\lambda \phi(\lambda)}$$

where $\phi(\lambda)$ represents the energy-wavelength distribution of the incident light. Over a wavelength range such that changes in f and n are small, K is independent of $\lambda$. Hence,

$$T = \frac{\sum_\lambda e^{-d_\lambda} \, \phi(\lambda)}{\sum_\lambda \phi(\lambda)} - K\frac{\sum_\lambda d_\lambda \, e^{-d_\lambda} \, \phi(\lambda)}{\sum_\lambda \phi(\lambda)} \quad \ldots(5)$$

The first term of (5) represents the transmission expected on the basis of the Lambert-Beer law; the second term is a relatively small correction factor introduced by the failure of the optical system to collimate perfectly the light passing through the absorption cell.

The percentage change in the transmission associated with a change $\Delta p$ in the source-to-lens distance, and a corresponding change of $\Delta K$ in K is very nearly

$$100 \, \Delta K \, \frac{\sum_\lambda d_\lambda \, e^{-d_\lambda} \, \phi(\lambda)}{\sum_\lambda e^{-d_\lambda} \phi(\lambda)} \quad \ldots\ldots\ldots\ldots\ldots(6)$$

Since the corresponding expression for monochromatic light is

$$100\ \Delta K\ d_{\lambda}$$

it is apparent that the changes in transmission with p occur in the same way whether monochromatic light or a wavelength band of finite width is used.

## Introduction.

The leading feature of the theory outlined above is that the variation of the measured transmission of a solution with change in the source-to-lens distance is very small, even though the source-to-lens distance be varied from one to three or four times the focal length of the lens. The importance of this leading feature, from the viewpoint of instrument design is sufficient to warrant an experimental investigation to ensure that no major factor has been overlooked in the theory.

The investigation described in the following pages, involved the measurement of the transmission of a certain solution, as the source of light (a slit) was moved away from the 'collimating' lens and absorption cells. The experimental variation of the transmission has been compared with the variation expected from theory.

## Apparatus.

The apparatus is shown diagrammatically in fig. 5. It permitted an investigation of changes in the measured transmission of a solution as the distance between the light source and collimating lens was varied.

An image of a 32 volt, 100 watt inside frosted tungsten lamp U was formed by means of a lens M on a screen containing a slit S. The light passed through a compensating cell, W or W', and through a red glass filter F. Light from the slit was received by the collimating lens L, whose aperture was limited by a circular diaphragm D; it then passed through an absorption cell, C or C', and was finally incident on a barrier layer photocell P. The compensating cell W and the absorption cell C contained aqueous copper sulphate solution, while the cells W' and C' contained distilled water. Sliding mounts permitted either of the compensating cells or either of the absorption cells to be inserted in the light beam. The collimating lens, absorption cells and photocell were mounted on a single base and could be moved as a unit along the optic axis of the system. All other components of the system were fixed.

The lamp U was operated from a double bank of

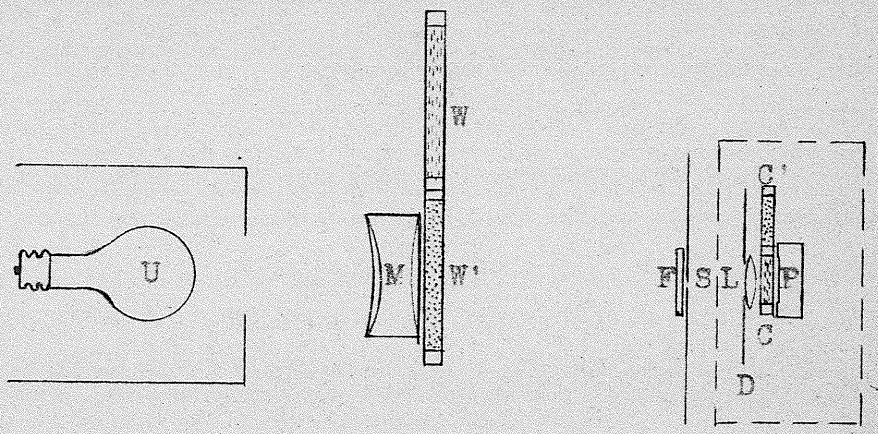


Fig. 5. Diagram of Apparatus.

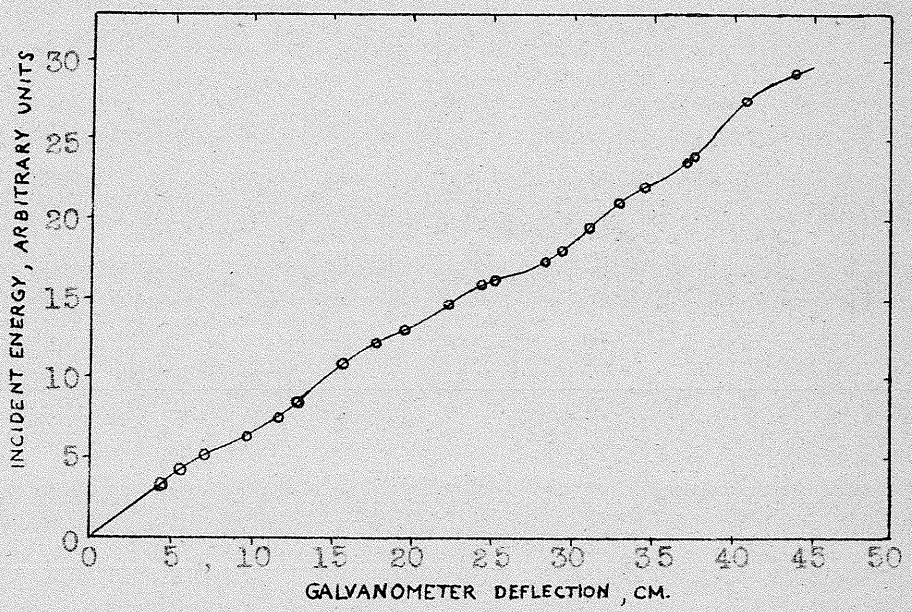


Fig. 6. Relation between galvanometer deflection and light energy incident on the photocell.

storage batteries. After a preliminary running period, repeated checks of the photocell response over a half-hour interval showed no variations that could not be attributed to experimental error in reading galvanometer deflections. The condensing doublet M had a 10 cm. diameter and a 10 cm. effective focal length. These characteristics were required in order that the lamp image should extend beyond the ends of the slit and that the diverging ray bundle should completely fill the collimating lens at all times. Characteristics of the filter F are given in fig. 7. The slit was 3.4 cm. long and 1 mm. wide. The "Photronic" cell P was connected to a galvanometer of sensitivity $2.2 \times 10^{-9}$ amp. per mm. The internal depths of the compensating and absorption cells were respectively 0.83 and 0.68 cm.

Investigations were carried out with two different lenses, (a) a 5 cm. f:1.25 lens, and (b) a 10 cm. f:2.5 lens. Lenses of high light-gathering power were chosen, since according to the theoretical analysis they are associated with more marked changes in the transmission value on altering the slit-to-lens distance. For a similar reason a high concentration of copper sulphate was used in the absorption cell, viz. 1.0 M.; this solution transmitted about 2% of the

filtered light incident upon it. The concentration of the copper sulphate in the compensating cell, W, was adjusted so that approximately equal deflections were obtained when W and C' were substituted for W' and C. This was done for the following reasons: (a) in order that both deflections should be sufficiently large for accurate reading; (b) to obviate calibration of the photocell-galvanometer system over a wide range of incident intensity; and (c) To ensure that the wavelength distribution of the light on the photocell remained essentially constant.

## Experimental Procedure.

The following procedure was adopted in making a measurement. The collimating lens was fixed at a given distance from the slit. The galvanometer deflection was noted with compensating cell W' and absorption cell C in the light beam. Cells W and C' were then inserted and the deflection was again noted. The deflections were converted into terms of energy incident on the photocell by means of a calibration curve (cf. fig. 6). The ratio of these energies was proportional to the transmission of the copper sulphate solution. This procedure was repeated with the

collimating lens at various distances from the slit; the range covered extended from one to three or four times the focal length of the lens (cf. Tables I to III).

The relation between galvanometer deflection and energy incident on the photocell was determined for the wavelength band used in the experiments with a precision considerably higher than that attained in the actual measurements of transmission. The slit S was removed and the condensing doublet M was replaced by a 10 cm. f:2.5 lens, whose aperture was varied in a known manner, by means of a series of stops of accurately known dimensions. The calibration curve is shown in fig. 6, in a very reduced scale.

The variation of the transmission of the filter F with wavelength was determined experimentally by the following method. An incandescent lamp was placed about 50 cm. from the slit of a spectroscope equipped with a wavelength scale. Light through the upper half of the slit passed through the filter, while the light intensity through the lower half was reduced by means of a rotating variable sector. The transmission of the filter was determined by adjusting the sector to a given transmission, and then observing visually the wavelength at which the line of

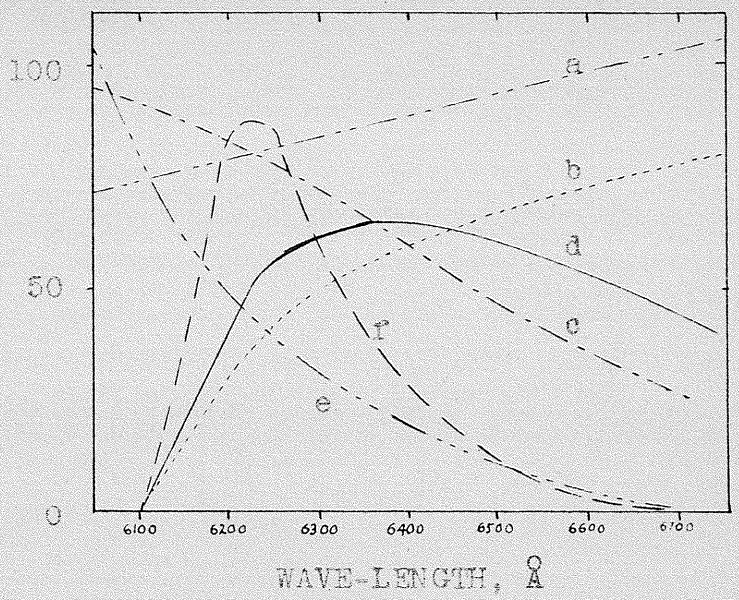


Fig. 7. (a) Energy distribution of radiation emitted by a tungsten filament at 2600°K. (1), together with emission coefficients of tungsten; (b) determined transmission curve for the filter; (c) sensitivity curve for the photocell (2); (d) 'effective' energy distribution, ø, viz. the products of ordinates of curves a, b, and c; (e) transmission curve for a 1.0 M aqueous copper sulphate solution in a cell of depth 0.68 cm. (3); (f) response curve for the photocell, viz. the products of ordinates of curves d and e. All ordinates are in arbitrary units. It appears from consideration of curve f, that about 75% of the photocell response in these experiments was attributable to radiation in the wavelength range 6150—6350 Å.

1. International Critical Tables. McGraw-Hill Book Co., New York, vol. 5, pp.238-242. 1929.

2. Weston Electrical Instruments Corp. Technical data Sheet. 1938.

3. International Critical Tables, vol. 5, p.330. 1929.

separation between the light which passed through the sector and the light which passed through the filter disappeared. The transmission curve of the filter appears in fig. 7.

## Results

Typical results for two lenses of different focal length are given in Tables I and II. Results obtained when light was permitted to pass only through the peripheral portion of the collimating lens are given in Table III. A 1.0 M copper sulphate solution and a slit length of 3.4 cm. were used throughout the experiments.

The values given in the second column of each table represent the averages of two sets of observations. They were obtained by multiplying the determined ratios of the energies incident on the photocell by 0.02; this corrected for the effect of the compensating cell, which transmitted about 2% of the incident light. Accordingly, the absolute values of the transmission are approximate, but the relative values are good to better than 0.4%. The third column of each table gives the percentage change in the transmission.

Calculated values for the percentage change in transmission are given in the fourth column of each table. These involve the evaluation of equation (6) for the conditions of the experiments. An effective value for $\Sigma_\lambda\ e^{-d_\lambda}\ \phi(\lambda)$ was determined by summing graphically over the range 6000 to 6800 Å the product of the ordinates of the curves for lamp emission, filter transmission, photocell response, and copper sulphate transmission (cf. fig. 7). In a similar way, a value for $\Sigma_\lambda\ d_\lambda\ e^{-d_\lambda}\ \phi(\lambda)$ was obtained from the curves mentioned above, together with the optical density curve for the copper sulphate solution. The expected percentage changes in transmission of the copper sulphate solution were then calculated from expression (6), using equation (4a) to evaluate $\Delta K$. These changes are about 60% of the changes expected for monochromatic light transmitted through a solution of equivalent optical density.

Table I.

Focal length of lens, 10 cm.; aperture 3.2 cm.

| Distance from slit to lens p, cm. | Observed transmission, T | Percentage change in transmission | |
|---|---|---|---|
| | | Observed | Calculated |
| 10.0 | 0.01992 | -0.4 | -0.3 |
| 12.0 | 0.01998 | -0.1 | -0.1 |
| 14.0 | 0.02000 | 0.0 | 0.0 |
| 16.0 | 0.02000 | 0.0 | 0.0 |
| 18.0 | 0.02000 | 0.0 | 0.0 |
| 20.0 | 0.02000 | 0.0 | 0.0 |
| 22.0 | 0.02002 | +0.1 | 0.0 |
| 24.0 | 0.02000 | 0.0 | 0.0 |
| 26.0 | 0.02000 | 0.0 | 0.0 |
| 28.0 | 0.01998 | -0.1 | -0.1 |
| 30.0 | 0.01998 | -0.1 | -0.1 |

Table II.

Focal length of lens, 5.0 cm.; aperture, 3.2 cm.

| Distance from slit to lens p, cm. | Observed transmission T | Percentage change in transmission | |
|---|---|---|---|
| | | Observed | Calculated |
| 5.0 | 0.02012 | -0.5 | -0.8 |
| 5.5 | 0.02024 | -0.4 | -0.4 |
| 6.0 | 0.02020 | -0.1 | -0.2 |
| 6.5 | 0.02024 | ∱0.1 | -0.1 |
| 7.0 | 0.02016 | -0.3 | 0.0 |
| 7.5 | 0.02024 | ∱0.1 | 0.0 |
| 8.0 | 0.02024 | ∱0.1 | 0.0 |
| 8.5 | 0.02018 | -0.2 | 0.0 |
| 9.0 | 0.02020 | -0.1 | 0.0 |
| 9.5 | 0.02012 | -0.5 | 0.0 |
| 10.0 | 0.02016 | -0.3 | 0.0 |
| 10.5 | 0.02024 | ∱0.1 | 0.0 |
| 11.0 | 0.02024 | ∱0.1 | 0.0 |
| 11.5 | 0.02020 | -0.1 | 0.0 |
| 12.0 | 0.02016 | -0.3 | -0.1 |
| 12.5 | 0.02016 | -0.3 | -0.1 |
| 13.0 | 0.02014 | -0.4 | -0.2 |
| 13.5 | 0.02028 | ∱0.3 | -0.2 |
| 14.0 | 0.02026 | ∱0.2 | -0.2 |
| 14.5 | 0.02020 | -0.1 | -0.3 |
| 15.0 | 0.02018 | -0.2 | -0.3 |
| 15.5 | 0.02018 | -0.2 | -0.3 |
| 16.0 | 0.02022 | 0.0 | -0.4 |
| 17.0 | 0.02020 | -0.1 | -0.4 |
| 18.0 | 0.02016 | -0.3 | -0.5 |
| 19.0 | 0.02016 | -0.3 | -0.5 |
| 20.0 | 0.02014 | -0.4 | -0.6 |

Table III.

Focal length of lens, 5.0 cm.; aperture 3.2 cm.; central opaque stop of 2.2 cm. diameter.

| Distance from slit to lens p, cm. | Observed transmission T | Percentage change in transmission | |
|---|---|---|---|
| | | Observed | Calculated |
| 5.0 | 0.02008 | -0.2 | -1.0 |
| 5.5 | 0.02000 | -0.6 | -0.6 |
| 6.0 | 0.02000 | -0.6 | -0.2 |
| 6.5 | 0.02000 | -0.6 | -0.1 |
| 7.0 | 0.02008 | -0.2 | 0.0 |
| 7.5 | 0.02012 | 0.0 | 0.0 |
| 8.0 | 0.02010 | -0.1 | 0.0 |
| 8.5 | 0.02012 | 0.0 | 0.0 |
| 9.0 | 0.02014 | +0.1 | -0.1 |
| 9.5 | 0.02010 | -0.1 | -0.1 |
| 10.0 | 0.02018 | +0.3 | -0.2 |
| 10.5 | 0.02004 | -0.4 | -0.2 |
| 11.0 | 0.02000 | -0.6 | -0.3 |
| 11.5 | 0.01992 | -1.0 | -0.4 |
| 12.0 | 0.02000 | -0.6 | -0.5 |
| 13.0 | 0.01994 | -0.9 | -0.6 |
| 14.0 | 0.01988 | -1.2 | -0.7 |
| 15.0 | 0.01988 | -1.2 | -0.9 |
| 16.0 | 0.01992 | -1.0 | -1.0 |
| 17.0 | 0.01982 | -1.5 | -1.1 |
| 19.0 | 0.01980 | -1.6 | -1.3 |
| 20.0 | 0.01986 | -1.3 | -1.4 |

## Discussion and Conclusion.

The data of Tables I and II show that the observed transmission of the solution varied by less than the experimental error of measurement (0.4%), even though the lens-to-source distance was increased from one to three or four times the focal length of the lens. The data of Table III exhibit a detectable variation in the transmission; the trend is in the direction expected from theoretical considerations. While an accurate check of individual calculated values has not been practical because of the high precision of measurement involved, the data furnish strong support for the chief prediction of the theory, viz., that with the optical system described, the source of light may be placed at a considerable distance from the principal focus of the collimating lens without introducing serious errors in determined transmission values.

Acknowledgments.

The author wishes to express his appreciation for the assistance which has made possible the carrying out of the experimental work described in this thesis, to the following institutions and individuals:

to the Physics Department of the University of Manitoba who granted the use of apparatus and other facilities.

to the National Research Council of Canada, who gave financial assistance, in the form of a $250 Bursary.

to Dr. G. O. Langstroth of the Department of Physics of the University of Manitoba, who suggested the problem and supervised the work.

to Dr. M. W. Johns of Brandon College, to Mr. R. Bird of the University Workshop, and to Mr. R. M. Smith, who aided in the construction of the microphotometer.

# Appendix I.

## Early History of Spectroscopy.

The foundations of modern spectroscopy were laid about 1859 by Bunsen and Kirchoff. Their work and that of subsequent investigators showed that the line spectra, such as first observed by Herschel in 1822, were determined by the materials in the source. Detailed studies of the light emitted by different elements followed. The spectral lines emitted by the elements were linked with the dark lines found by Fraunhofer in the spectrum of sunlight. Foucault, in 1849 observed similar dark lines, when light from an arc was passed through a flame containing sodium vapor. Subsequently, Kirchoff published his absorption laws explaining the phenomenon.

Along with the studies of the characteristic spectra of the elements, work has proceeded on the measurement of wavelength, and on the extension of the range of wavelengths studied to the ultra violet and infra red regions of the spectrum. The study of characteristic spectra has been aided by improvements in prism instruments, and by the introduction of large gratings which are capable of very high dispersion. The absolute measurement of wavelength, begun by Fraunhofer, was improved by Rowland with better diffraction gratings, and has lately been carried to high precision by the use of the interferometric methods of Fabry and Perot and of Michelson.

Attempts to deduce some relation between the spectral lines of an element were not successful, until Balmer as a result of his studies of the hydrogen atom spectrum was able to express the wavelengths of the nine known hydrogen lines by means of a series relation. Balmer's formula was generalised by Rydberg, whose formula agrees fairly well with the experimental results, small systematic errors being present, however.

The first successful explanation of spectral series of a theoretical nature was put forward by Bohr. Bohr's theory was based on the atom proposed by Rutherford, consisting of a positively charged nucleus comprising almost the whole mass of the atom, and a number (atomic number of the atom) of electrons which moved in circular orbits around the nucleus. The possible orbits were determined by the condition that the (angular momentum) of the electron be an integral multiple of $h/2\pi$. The atom emits or absorbs energy whenever an electron 'jumps' from an outer orbit to an inner, or vice versa. This theory was modified by Sommerfeld, who assumed that elliptic orbits were possible. A further modification came with the assumption that the electron may have a 'spin' about its centre of gravity. These theories lead directly to the vector model of the atom (cf. Appendix II).

The failure of classical mechanics in the treatment of atomic phenomena is evidenced by the inability of the Bohr theory and its modifications to allow of the prediction of the energies required to remove an electron from neutral helium or from other more complicated atoms or ions and much more. Of the later theories replacing that of Bohr, Heisenberg's matrix mechanics was the first to appear. This theory was developed further by the work of Born, Jordan and Dirac. Shortly after, wave-mechanics, invented originally by deBroglie to treat the phenomenon of the wave-like properties exhibited by electrons, was applied by Schrödinger to other material particles. Matrix mechanics and wave mechanics have been shown to be equivalent, and both permit the calculation of values for the energy levels, though the calculation is somewhat abstruse and laborious.

# Appendix II.

## Spectroscopic Nomenclature.

The following presents a scheme which permits a simple qualitative description of the atomic energy states. In Bohr's theory of the atom, discrete energy values entered (cf. Appendix I) which can be stated in terms of integral multiples of an angular momentum. These integers are called quantum numbers. Further quantum numbers arise in the extension of Bohr's theory to include elliptic orbits and electron spin. Since these quantum numbers have vectorial properties, this method of describing the energy states is termed the 'vector model'. In the case of atoms having a large number of extra-nuclear electrons, the inner electrons form 'completed shells' and may usually be regarded as merely shielding the nucleus; only the actions of the outermost 'optic' or valence electrons need be considered.

A list of the quantum numbers used, and their significance follows:

1. the principle quantum number, n, is associated with the average distance of the electron from the nucleus. n takes values 1, 2, 3, ...

2. the azimuthal quantum number, $l$. In the case of an elliptical orbit (the nucleus occupies one focal point of the ellipse), if the average radial momentum of the electron be multiplied by the total amount by which the radius changes

during one transit of the orbit (adding both increase and decrease), a quantity is obtained which is set equal to $n_r$ h. $n_r$ is called the radial quantum number and takes values 0, 1, 2, ... Then, the total quantum number of the orbit, $n = (\ell \neq 1) \neq n_r$, where $(\ell + 1) = k$ is called the azimuthal quantum number, and takes values 0, 1, 2, ... $\ell$ is always less than n, however.

3. the spin quantum number, s. The spin momentum is written $sh/2\pi$, where $s = \pm \frac{1}{2}$, according as the spin momentum vector is (parallel or antiparallel) to the vector $\ell$ representing the angular momentum (not physically) of the electron in its orbit.

4. the total angular momentum of an atom with one optical electron (e.g. hydrogen, alkali metals) is given by j, where $j = \ell \neq s$

5. the total azimuthal quantum number of an atom with two optical electrons is L, where $L = \ell_1 \neq \ell_2$, the quantities being added vectorially.

6. the total spin quantum number of an atom with two optical electrons is S, where $S = s_1 \neq s_2$.

7. the total angular momentum of an atom with two optical electrons is J, where $J = L \neq S$. This type of coupling is called Russel and Saunders coupling, or simply L-S coupling.

8. Selection principles. The following rules, determined empirically permit the prediction of the transitions which can take place and of transitions which are unlikely to take place. They are not absolutely rigorous, and exceptions to them have been observed.

(i) the change in L is $\pm 1$. if one electron changes orbit

(ii) S does not change.

(iii) the change in J is 0 or $\pm 1$.

9. Designation of terms. A particular energy level is denoted by an expression of the form $M^{m}L_{J}$, where M is an integer depending on N (M is not necessarily equal to N); m denotes the multiplicity of the level, i.e. singlet, doublet, etc.; L is S, P, D, or F according as L is 0, 1, 2, or 3, (the letters S, P, D, and F refer respectively to the Sharp, Principle, Diffuse, and Fundamental Series); J is a number.

10. Designation of transitions. A transition is denoted by an expression of the form $M'^{m'}L'_{J'}-M''^{m''}L''_{J''}$, where the ' values refer to the final level of the electron, and the " values to the initial level. Note that the changes in the quantities are limited by the selection rules given above in (8).

# Appendix III.

## Notes on Modern Methods of Quantitative Spectrographic Analysis.

Preparation of Samples.

The first step in the procedure is the preparation of the samples. The procedure depends to some extent on the type of material to be analysed, the source to be used, and the precision required. Samples of conducting materials may be used as the electrodes of a spark or arc. Non-conducting materials may be placed in a cavity in an arc electrode; or they may be dissolved, by chemical treatment if necessary, and so obtained in the form of a solution. The analysis of solutions presents a number of alternatives: a definite amount of the solution may be placed on the prepared electrode of a spark[19]; the sparking may take place between two jets of the solution[20]; or the solution may be sprayed into a flame[21]. Of these, the last two methods are limited to cases where a relatively large amount of material is available, and the last method limits the scope of the analysis to elements capable of being excited in a flame.

19. McRae, D.R., Langstroth, G.O., and Foster, J.S., Proc. Roy. Soc. A, 165:465-473. 1938.

20. Duffendack, O.S. and Thomson, K.B., Proc. Am. Soc. Testing Materials, 36:301. 1926.

21. Lundegardh, H., Lantbruks. Hogskol. Ann., 3:49. 1936.

Excitation of Samples.

The most common sources used in spectroscopic work are electrical discharges. Flames have been used, but are not satisfactory, since they operate at relatively low temperatures, and in general are suitable only where the atoms to be investigated are easily excited. Among the types of electrical discharges used are condensed and uncondensed a-c sparks, d-c sparks, high frequency sparks, stationary arcs, rotating arcs and interrupted arcs. Sources which operate with a high applied potential and relatively cool electrodes are classified in general as sparks, while sources which operate with comparatively high electrode temperatures usually at relatively low potentials are classified as arcs.

The operation of an arc is characterised by the formation of a hot spot on the cathode, which gives off a copious supply of electrons. These are accelerated towards the anode, and their collisions with the atoms and molecules in the inter-electrode space raises the temperature, and produces further ions to aid in the carriage of the discharge. Arcs can be run at potentials from 60 to 220 volts and temperatures in the arc range from 1000 to 6000$^{o}$C. For most work

only a small portion of the arc is used as a source, the arc being focussed by means of a condensing lens on the slit of the instrument used to obtain dispersion. By diaphragms reducing the length of the slit the continuous spectrum emitted by the hot electrodes can be eliminated and any desired portion of the arc used as a source. Although the arc has been much used in spectroscopic analysis, there is some disagreement among workers in the field on the score of its reproducibility, and claims that arc sources are more sensitive are not generally accepted.[7]

The characteristics of a spark are largely dependent on the electrical circuit. The A circuit used commonly in spectroscopic work is the condensed form of a-c spark. This form has been used in the experiments described in Part A, and the circuit has been indicated in fig. 1. The discharge from such a circuit ordinarily has three phases; these come about as follows. The condenser C (cf. fig. 1) charges up to a high potential such that the resistance of the air in the spark gap breaks down. The discharge builds up during the ignition phase, and then takes a form similar to the glow discharge observed in Geissler tubes. The ions formed strike the cathode causing a small localised 'hot spot',

which forms a source of electron emission. At this stage, the discharge changes from the glow phase into a form operating at relatively low potential and similar to that found in the d-c arc. These three types of discharge are present in each half cycle, the resulting potential-time distribution being similar to that indicated in fig. 8. The period of such a spark is ordinarily of the order of $10^{-5}$ to $10^{-7}$ seconds, and there are as a rule between 20 and 30 oscillations to every half-cycle of the input. From an inspection of equationm1, it can be seen that an increase in the inductance L will lengthen the period of each discharge, and since the time taken in the ignition and glow phases is practically independent of the period, this will result primarily in a lengthening of the arc phase. The ignition phase produces strong air spectra, while the arc phase produces strong spectra of the electrode materials, and any materials which may be on the electrodes. By varying the inductance in the circuit, then, the relative importance of ignition and glow phases over the arc phase can be decreased or increased, thus enabling a spectrum to be obtained to meet the requirements of the work in hand.

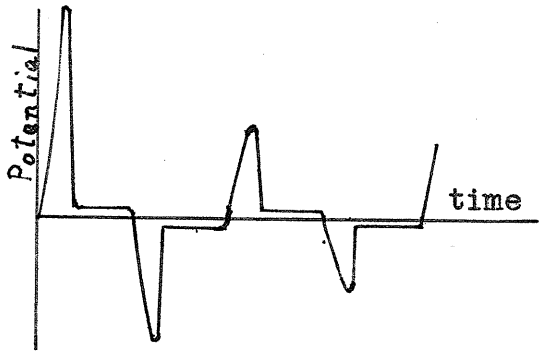


fig. 8.

Dispersion-Producing Instruments.

The description and theory of the standard instruments used for dispersing the light emitted by the source, such as spectroscopes, and spectrographs of prism and grating types, are to be found in any standard book on advanced optics. For that reason, they will not be discussed here. However, a brief description of the 'medium' quartz spectrograph used in the experiments described in Part A , and the methods of putting the instrument into adjustment are to be found in Appendix IV.

Measurement of the Intensity of Spectral Lines.

Photoelectric and visual methods have been used for the direct measurement of line intensity. Limitations are imposed on such methods, however, by the low intensity of the spectral lines under investigation, by the complexity of the spectrum, and for visual work, by the fact that the persistent lines of many elements lie in the ultra violet region of the spectrum.

Photographic plates are in general use for the recording of spectra, since they suffer from none of the

limitations noted above. The photo-plate is an integrating device, and consequently spectral lines of low intensity merely require a longer exposure; the resolving power of a photo-plate is good; special plates are now available, so that the spectral region from 1200 Å to 7000 Å can be studied.

A discussion of photographic plates, with reference to the errors their use may introduce into quamtitative work is to be found in Appendix V.

The earliest method of measuring relative intensity from a photographic plate utilised an optical wedge of grey glass placed before the slit of a stigmatic spectrograph. Thus a uniformly graded density was obtained for each spectral line. For two lines of nearly equal wavelength, the intensities which just fail to produce a silver deposit on the photo-plate will be equal, and the difference between the lengths of the lines will be a measure of the relative intensity of the lines. The weakness of this method lies in the difficulty of determining accurately the points of zero silver deposit.

Another method, similar in principle, is the use of a logarithmic sector. The relative intensity is measured in the same way, and suffers from the same difficulties.

The comparison methods, employing calibration marks produced by the aid of a step sector in front of the slit of a stigmatic spectrograph have been described in the Introduction to Part B.

# Appendix IV.

## Description, Theory and Adjustment of the Spectrograph.

Description of the Spectrograph.

The spectrograph was built in the University of Manitoba Workshop. It appears in the upper right of Plate I and in Plate V. It is comparable to the commercial 'medium' quartz spectrograph in size and performance. The optical components consist of two 60 cm. f:12 uncorrected plano-convex quartz lenses, a 60° Cornu type quartz prism, and a slit whose width can be varied up to 3 mm. with a maximum length of 1.9 cm. The prism has faces 5.0 cm. long and 4.0 cm. high.

The base of the instrument is made up of two pieces of channel iron welded together. The slit and shutter assembly is mounted on a tube which slides and rotates in a collar, allowing longitudinal and rotational adjustments of the slit. The collar is securely mounted on an upright attached to the base.

The lenses and prism are mounted on a table which is securely fastened to the base. The lenses are mounted in supports which move in ways parallel to the optic axis of the system; the prism has a rotational movement. The arrangement of the optical train is shown in Plate VI.

The plate holder is of standard type, fitted with dark slide, and opening from the rear for loading purposes.

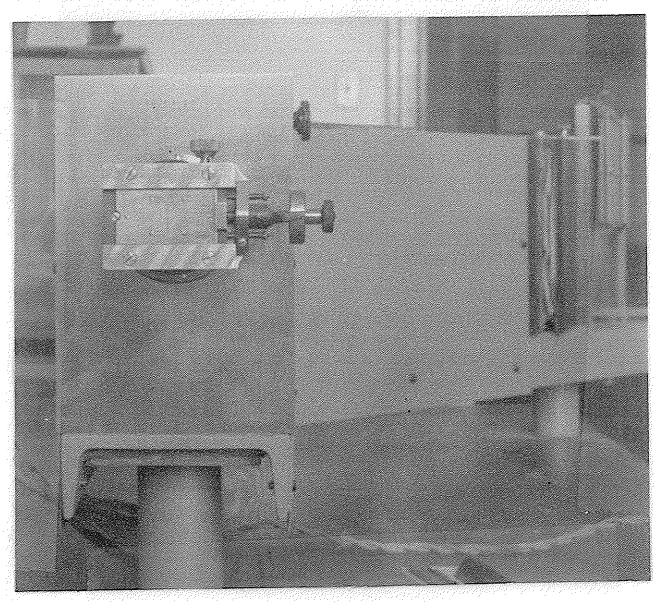

Plate V.

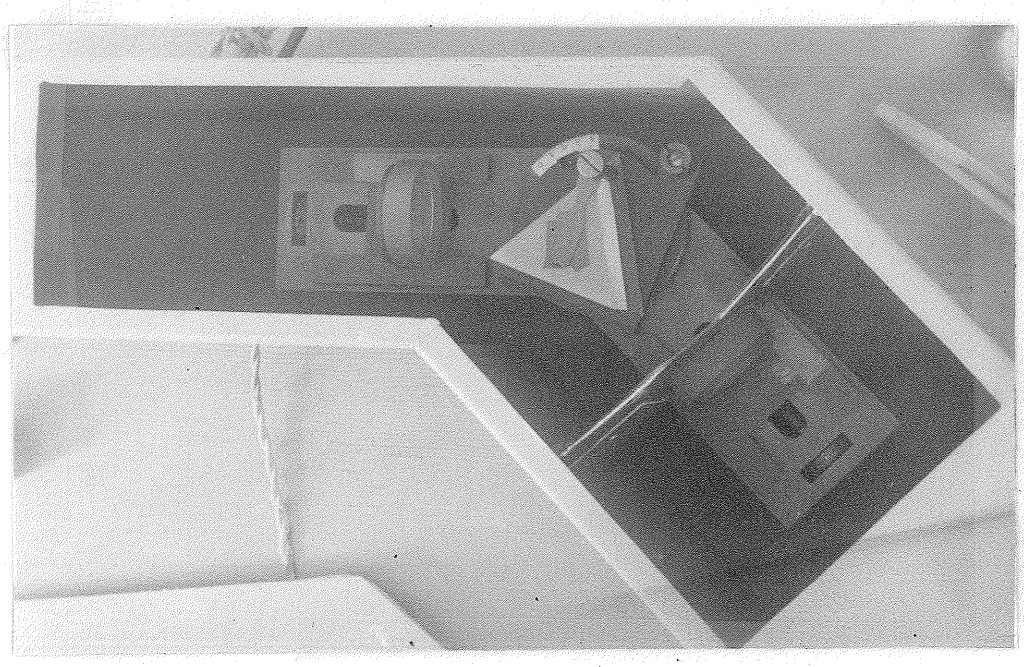

Plate VI

It slides in vertical ways in the plate holder mounting, and is moved by means of a rack and pinion. The plate holder mounting rotates on a bearing set into the base of the spectrograph, thus providing adjustment for the tilt of the plate. In order to correct for the curved focal plane of the slit images forming the spectrum, the plate holder is equipped with 'shims' against which the photographic plate rests. The method of determining these shims is described in following pages.

All adjustments are provided with scales, and wherever advisable, they have been equipped with a means of clamping in position. These provisions ensure that once in adjustment, the spectrograph will always be ready for use, and if at any time changes in the adjustment are made for any reason, the instrument can be readily returned to its original setting.

Leakage of light is prevented by a galvanised iron cover which fits over the instrument, and is screwed to the base and uprights at each end, and also by a leather bellows connecting the plate holder mounting to the upright at the camera end of the instrument. A further precaution is taken in the use of felt strips around the edges of the cover. Accession to the lens and prism assembly is provided by means of a lid which fits into the cover, immediately above this assembly.

Theory of the Spectrograph.

In fig. 9a, S represents the slit of the spectrograph and Q the slit image formed by the lens system consisting of the collimating lens C and the camera lens T. Q' is the image of the slit formed by C. The distances are as indicated in the figure. Applying the simple lens formula to each of the two lenses, eliminating q' and solving for q,

$$q = \frac{f\{pf - j(p-f)\}}{pf + (f-j)(p-f)} \quad \ldots\ldots\ldots\ldots\ldots\ldots (7)$$

where f is the focal length of the lenses.

From fig. 9b, the deviation $\delta$ of light passing through a $60^\circ$ prism of refractive index $\mu$ for light of wavelength $\lambda$ is given by

$$\delta = i' + i'' - 60^\circ$$

We also have from the definition of refractive index

$$\mu = \frac{\sin i'}{\sin r'} = \frac{\sin i''}{\sin r''}$$

Eliminating r', r'' and i'' from these two equations,

$$\delta = i' - 60^\circ + \sin^{-1}\left\{\frac{\sin i' + \sqrt{3(\mu^2 - \sin^2 i')}}{2}\right\} \ldots (8)$$

The perpendicular distance of the slit image formed by light of wavelength $\lambda$, from the optic axis of the slit-

collimating lens system is given by d (fig. 9c), where

$$d = (q \nearrow \tfrac{1}{2}j) \sin\delta \quad \ldots\ldots\ldots\ldots\ldots\ldots (9)$$

The position of a spectral line of given wavelength is now completely determined, since, knowing the value of $\mu$ for a given wavelength $\lambda$, $\delta$, $(q \nearrow \frac{1}{2}j)$ and d can be evaluated, by means of the equations (7), (8) and (9). A value of p is taken, such that the slit is at the principal focus of the lens C for a line of intermediate wavelength $\lambda$ (f is a function of $\mu$ and hence of $\lambda$). The angle i' takes a value such that the prism is at minimum deviation for the intermediate wavelength, viz.

$$i' = \sin^{-1}\left\{\frac{\mu \sin 60^\circ}{\sqrt{2 \cos 60^\circ}}\right\} \quad \ldots\ldots\ldots\ldots\ldots\ldots (10a)$$

$$= 2i' - 60^\circ \quad \ldots\ldots\ldots\ldots\ldots\ldots\ldots\ldots (10b)$$

The position of the entire spectrum can now be determined to a first approximation by evaluating $\delta$, $(q \nearrow \frac{1}{2}j)$ and d for two extreme values of $\mu$ and $\lambda$. (cf. fig. 10c).

The spectrograph was built to conform to the dimensions obtained as outlined in the above; the final adjustments to correct for the curved focal plane of the slit images forming the spectrum were made empirically, as described below.

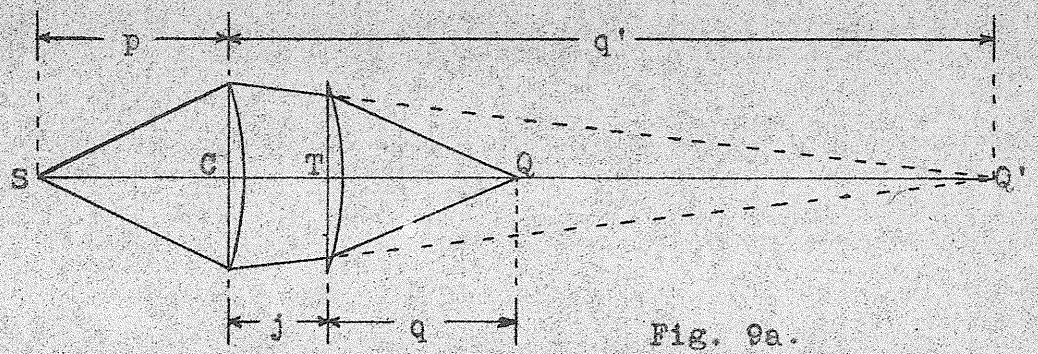


Fig. 9a.

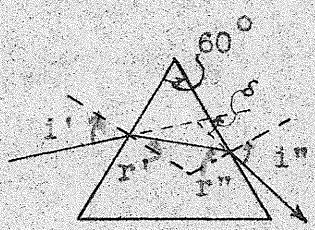


Fig. 9b

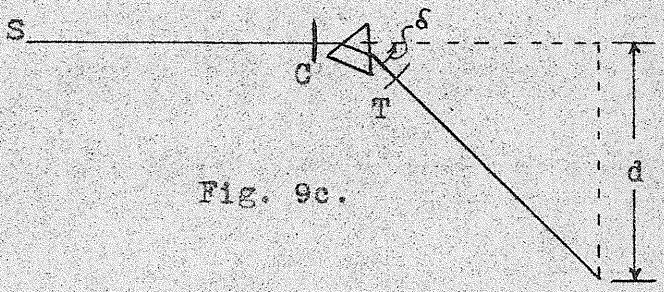


Fig. 9c.

Fig. 9. Theory of the Spectrograph.

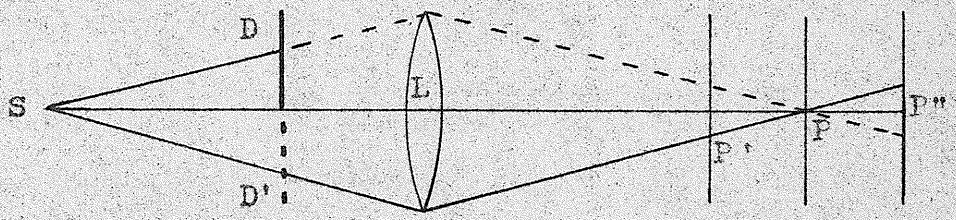


Fig. 10a.

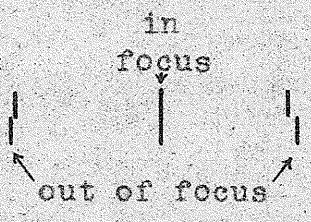


Fig. 10b.

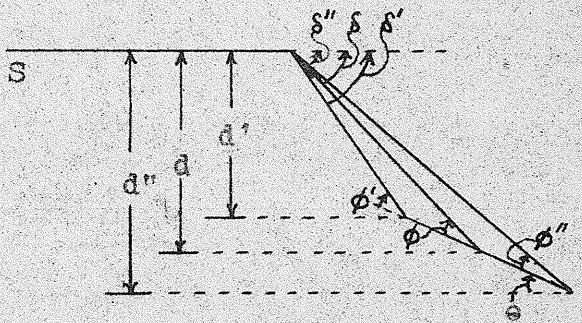


Fig. 10c.

Fig. 10. Adjustment of the Spectrograph.

Adjustment of the Spectrograph.

The slit images formed by the optical system of a spectrograph ordinarily lie in a curved surface. For an instrument of the size and spectral range (2100 to 6000 Å) of the spectrograph here described, the effects of a curved focal plane are appreciable. Hence, the plate holder must be fitted with 'shims' against which the photographic plate can rest, ensuring that the lines will be in good focus from one end of the plate to the other. The following considerations entered into the preperation of the shims.

The Hartmann criterion for focus was used. The optics of the spectrograph can be considered equivalent to those indicated in fig. 10a, where S represents the slit, L the lens system, and P the slit image. If now, half of the lens is covered with a diaphragm D, and the plate is at P, the image will be unchanged; if, however, the plate is at P' or P", the image will only be half as wide as formerly. If the other half of the lens is covered with D', different halves of the image will be obtained at P' and P". Hence, the state of focus of the spectrum can be determined by taking two exposures, using neighboring portions along the length of the slit (by means of an occultor), and screening off alternate halves of the lens system. If a given line

is in focus, the two images will be directly in line (cf. fig. 10b); while, if the line is not in focus, the two images will be displaced one from the other.

The curve along which the plate must lie was determined by an examination of the change in the focal points of the spectral lines, with movement of the camera lens along the optic axis of the system; i.e. the change in $(j \not\sim q)$ with j. Putting $(j \not\sim q) = x$, differentiating equation (7) with respect to j in order to obtain dq/dj, and neglecting terms in $(p-f)^2$ since (p-f) is small with respect to p and f, it appears

$$dx = dj \quad \ldots\ldots\ldots\ldots\ldots\ldots\ldots\ldots\ldots\ldots (11)$$

Hence, the spectrum as a whole moves parallel to the optic axis with the camera lens. An arbitrary spectral line A is chosen, which is in good focus at an arbitrary setting of the camera lens. Exposures are taken, for a number of settings of the camera lens, two exposures being taken at each setting, each with a different half of the lens system covered. From these pictures, using the criterion previously described, the distances dx from the arbitrary point of the focal points of a number of lines over the spectral range are determined. It is now necessary to shape the shims so that all these lines are in good focus on the plate.

If the distance between the emulsion of the photographic plate and the point of good focus of a given line, be y, measured perpendicular to the plate, then, from fig. 10c,

$$y = dx \sin \phi = dj \sin (\delta - \theta) \quad \ldots\ldots\ldots\ldots (12a)$$

where

$$\theta = \tan^{-1}\left\{\frac{d'' - d'}{d'' \cot \delta'' - d' \cot \delta'}\right\} \quad \ldots\ldots\ldots (12b)$$

By the use of equations (12a) and (12b), and the values of dx determined, the values of y for the corresponding lines can be determined, and the shims constructed.

# Appendix V.

## Photographic Plates.

Manufacture and Treatment of photographic plates.

The photographic plate consists of a glass plate on which has been flowed a solution containing gelatine, silver bromide, and a little silver iodide. This solution is dried, forming the 'emulsion'. On exposure to light, the silver bromide is affected in some way, forming a 'latent image'. When the plate is placed in a solution containing reducing agents, the silver bromide is reduced, and metallic silver is deposited. The reducing agent must be of such a character as only to reduce the silver bromide which has been exposed to light, i.e. must have a reduction potential which lies between very narror limits. The developing agents are therefore limited; the two most common agents are hydroquinone and elon (monomethyl para-amino phenol sulphate); other agents used are pyrogallic acid, glycin-para-aminophenol, and diaminophenol. In addition to containing a reducing agent the developing solution must be alkaline; sodium carbonate is added to secure this. On exposure of the solution to air, the sodium carbonate would suffer oxidation, hence, sodium sulphite and sodium hyposulphite are added to retard this oxidation. Finally the speed of development is controlled by the addition of potassium bromide to the

developer. After development, the plate is immersed in a 'fixing' solution containing 'hypo' (sodium thiosulphate) in an (acetic) acid solution which arrests development at once. After fixing, the plate may be placed in a hardening bath of alum or formalin solution; the hardening produced in the gelatine guards against too easy scratching. Finally the plate is washed in water to remove the chemicals used in the previous processes. The washing is very important if the image is to be permanent.

Kinds of photographic emulsions.

Photographic emulsions of many varieties are available:

(i) high speed emulsions, that is emulsions which require only a relatively short exposure to light in order to produce the desired latent image. Such emulsions are usually objectionable on the ground of large 'grain'; this can be controlled somewhat by the use of 'fine grain' developer.

(ii) contrast. Contrast depends on the proportionality between the incident light and the amount of silver bromide affected.

(iii) sensitivity. The sensitivity of a plate depends on the wavelength of the incident light. Orthochromatic emulsions are sensitive in the yellow to green region of the spectrum. Panchromatic emulsions are sensitive up to 7000 Å. Emulsions are prepared which are sensitive up to about 12000 Å. For light of wavelength less than about 2000 Å, the gelatine absorbs very strongly. This difficulty can be overcome by dissolving the gelatine off with sulphuric acid, or by coating the plate with a fluorescent material. The fluorescent light from ethyl carboxylic ester of dihydrocollidine used in this way, will produce an image for incident light down to 580 Å. The ester must be dissolved off the plate with ethyl chloride before development. Schumann plates can be used, on which just enough gelatine is used to keep the silver bromide on the surface; these are very delicate.

Characteristic curves of a photographic plate.

The exposure E of a photographic plate is given by

$$E = I\,t \qquad \ldots\ldots\ldots\ldots\ldots\ldots\ldots\ldots\ldots\ldots (13)$$

where I is the incident light intensity and t is the exposure time. The density or 'blackening' of a silver deposit on a plate is measured by

$$D = \log_{10} i_o/i \quad \ldots\ldots\ldots\ldots\ldots\ldots\ldots\ldots (14)$$

where $i_o$ is the light intensity which falls on the silver deposit, and i is the transmitted intensity. The plot of D against log E results in a curve known as the characteristic curve of the plate. The form of the characteristic curve is indicated in fig. 11a. The exposure $E_o$ corresponding to X is called the 'inertia' of the plate. Exposure conditions are generally chosen so that the range of densities produced correspond to the straight (i.e. normal exposure) part of the curve. The form of the curve depends on the emulsion, developing process, and the wavelength of the light to which it was exposed. The slope of the straight portion is termed the 'contrast', denoted by $\gamma$ ($\gamma = \tan \phi$). The dependence of $\gamma$ on the development time t may be expressed by means of the relation

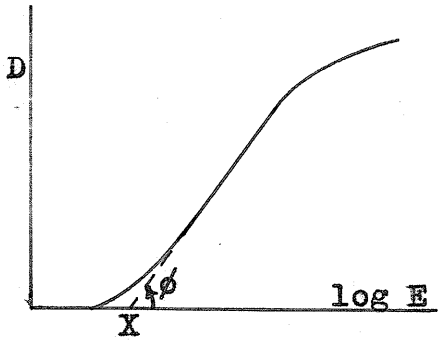


fig. 11a.

$$\gamma = \gamma_\infty (1 - e^{-kt}) \quad \ldots\ldots\ldots\ldots\ldots\ldots\ldots\ldots (15)$$

where k is a constant.

The speed of different plates is compared by means of the H. and D. (Hurter and Driffield) value given by $34/E_o$ ($10/E_o$ is sometimes used), or by means of Scheiner speeds, i.e.

the angular opening in a rotating sector necessary to produce a barely perceptible image under standard conditions.

The resolving power of a plate is determined as follows: Parallel lines ruled on a white sheet are photographed. The resolving power of the plate is then equal to the maximum number of lines per mm. which can be distinguished. (ordinarily from 38 to 160) The resolving power depends on the contrast, graininess and turbidity of the emulsion. Lines are broader for long exposures at high intensity, due to the scattering of light by the gelatine.

Reciprocity law failure.

It is found that equation (13) does not hold strictly. Schwarzschild's law states $I\, t^p$ = constant. However, p may be a function of I.

Intermittency effect.

An intermittent exposure does not in general produce the same blackening as a continuous exposure, even though the total exposure times be equal. If the frequency of interruption is more than about eighty per second, the intermittency effect vanishes.

Eberhard effect.

In the development of a plate, reaction products will accumulate at the area of greatest reaction, and the process is slowed down at such an area. In the case of spectral lines, this produces an effect such as indicated in fig. 11b. The broken line represents the ideal image while the continuous line represents the image obtained when Eberhard effect enters. The effect can be eliminated by developing for an 'infinite' time, i.e. until $\gamma$ approaches $\gamma_\infty$; and can be minimized by keeping the developer in constant agitation.

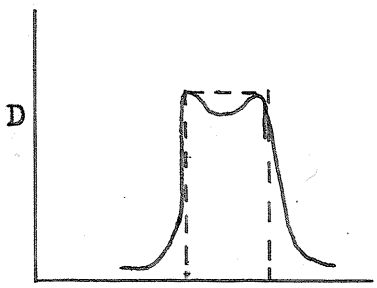


fig. 11b.

Solutions used to develop Eastman '40' Spectroscopic plates.

Elon-hydroquinone tray developer. Formula D-61a.

Stock Solution.

| | |
|---|---|
| Water, about 125°F. ..... | 500.0 cc. |
| Elon ..... | 3.1 gm. |
| Sodium sulphite (desiccated) ..... | 90.0 gm. |
| Sodium bisulphite ..... | 2.1 gm. |
| Hydroquinone ..... | 5.9 gm. |
| Sodium carbonate (desiccated) ..... | 11.5 gm. |
| Potassium bromide ..... | 1.7 gm. |
| Cold water to make ..... | 1.0 liter. |

For tray development, one part of stock solution is used to one part of water.

Acid hardening fixing bath. Formula F-5.

| | |
|---|---|
| Water, about 125°F. ..... | 1200.0 cc. |
| Sodium thiosulphate (hypo) ..... | 480.0 gm. |
| Sodium sulphite (desiccated) .... | 30.0 gm. |
| Acetic acid, 28% pure ..... | 96.0 cc. |
| Boric acid, crystals ..... | 15.0 gm. |
| potassium alum ..... | 20.0 gm. |
| Water to make ..... | 2.0 liters |

The hypo is dissolved in the warm water; then the other chemicals are added in the order named, dissolving each completely before adding the next; finally, cold water is added to make the volume required.

This bath remains clear and fixes clean until exhausted. Never attempt to restore an exhausted bath by adding hypo. Plates should be left in the fixing bath at least double the time it takes them to clear.

These formulas were obtained from the list of formulas supplied by the Eastman Kodak Company, Rochester, N. Y.